S8/02

HSCT Propulsion Airframe Integration Studies

Steve Chaney

The Boeing Company

- **Inlet Spillage Interference Analysis and Modelling**
  - ***** Lockheed Martin (Charlie Novak) *****
- **Supersonic Cruise PAI Drag Issues (Boeing)**
  - **CFD Validation, CFD/Test Comparisons**
  - **Bifurcated / Axisymmetric Inlet Drag Differences**

The Lockheed Martin spillage study was a substantial effort and is worthy of a separate paper. However, since a paper was not submitted a few of the most pertinent results have been pulled out and included in this paper. The reader is urged to obtain a copy of the complete Boeing Configuration Aerodynamics final 1995 contract report for the complete Lockheed documentation of the spillage work.

The supersonic cruise studies presented here focus on the bifurcated - axisymmetric inlet drag delta. In the process of analyzing this delta several test/CFD data correlation problems arose that lead to a correction of the measured drag delta from 4.6 counts to 3.1 counts. This study also lead to much better understanding of the OVERFLOW gridding and solution process, and to increased accuracy of the force and moment data. Detailed observations of the CFD results lead to the conclusion that the 3.1 count difference between the two inlet types could be reduced to approximately 2 counts, with an absolute lower bound of 1.2 counts due to friction drag and the bifurcated lip bevel.

Inlet Spillage Interference Analysis and Modelling

- **Data Analysis: NASA Ames Ref H 9x7 & 11 ft tests**
- **CFD Modelling: OVERFLOW**
  - **Isolated**
  - **Nacelle-in-Proximity**

1.0 INTRODUCTION

The technical objective of this study was to conduct analyses to determine effects of inlet oblique shock (nominal) spillage interference . This was done for nacelles in proximity to wing using force and pressure data obtained in NASA wind tunnel testing of a 2.7% scale model of the Boeing Reference H HSCT Configuration. Selected wind tunnel data were compared to computational fluid dynamics (CFD) analysis methods to determine if nominal spillage effects can be reliably predicted by CFD methods.

The technical approach taken during this study consisted of three parts. First the NASA-ARC Data Management System Utilities (CDDMS) were used to reduce the 2.7% Reference H Nacelle-Airframe Interference (NAI) wind tunnel data from tests conducted in both the 9'x7' and 11'x11' test facilities for:

isolated Mixed-Compression Translating Centerbody (MCTCB) nacelles,
isolated Bifurcated Two-Stage Supersonic Inlet (BTSSI) nacelles,
nacelle-to-nacelle interference with the MCTCB and BTSSI geometries,
nacelle-in-proximity to wing/body with the MCTCB, BTSSI and Ref. H geometries.

Second, and of equal importance to the data analysis, is the implementation of NASA-developed OVERFLOW CFD methodologies in analytical modeling. This was used to ensure prime/sub methodology compatibility and coordination. Emphasis was place on the modeling of the nominal spillage conditions for:

Mach numbers of 1.80 and 1.30,
MCTCB and BTSSI nacelle geometries,
isolated, nacelle-to-nacelle , and nacelle-in-proximity conditions.

As the final step in the approach, comparisons were made using CDDMS, FAST, PLOT3D and AcePlot to investigate CFD utility with respect of the accuracy and reliability in determining forces and surface static pressures.

MCTCB Compression System CFD Grid Topology

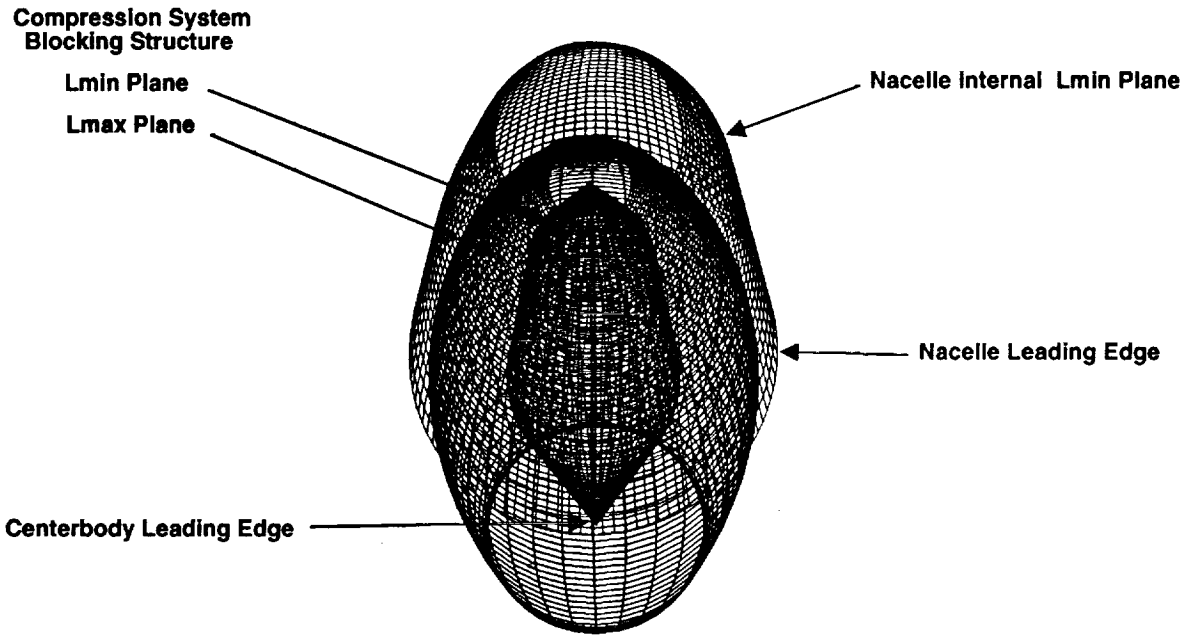

CFD Model(s) Development, MCTCB Compression System Gridding

Activities were also focused on developing compression system topologies, block overlapping strategies and viscous-spaced faces which would capture the spillage effects associated with the nacelles operating at nominal conditions using the OVERFLOW CFD methods. *Phantom* and *collar* grids where used to eliminated all *orphan points* with the PEGSUS code. Near-wall point spacing on the isolated MCTCB and BTSSI grids were held to 1.0E-03 and 1.0E-04 inches respectively in an effort to correctly describe the boundary layer growth on the ramp and the resultant shock displacement.

The MCTCB compression system geometry modeling was initiated first. An H-O topology was selected for the creation of a single block for each of the nacelles using the "K" direction as periodic . Overlapping at the leading and trailing edges of the centerbody were used to assure that the nominal spillage flowfield was captured. The singular axis typical to this type of topology was replaced by singular points at the leading and trailing edges of the centerbodies. When completed the grids were run through PEGSUS to develop the *"chimera"* or overlapping interpolants for subsequent OVERFLOW analysis. The MCTCB nacelle and Mach 1.8 centerbody surface grids shown in figure above resulted in PEGSUS-developed blocks with zero *orphan* points. The MCTCB centerbody grids were sized at 80 x 40 x 20.

Rapid translation of the MCTCB compression system position within the nacelle was made possible using the block translation/rotation/scaling feature within PEGSUS. That enabled the centerbody to be moved from design to off-design conditions with minimal grid/blocking modifications.

The following combined grids were developed with zero *orphan* points using PEGSUS:

- isolated MCTCB without compression system,
- isolated MCTCB with Mach 1.8 centerbody and outflow planes
- integrated Ref H/MCTCB with unstarted (Mach 1.2 setting) centerbodies and outflow planes,
- integrated Ref H/MCTCB with Mach 1.8 centerbodies and outflow planes.

BTSSI Compression System CFD Grid Topology

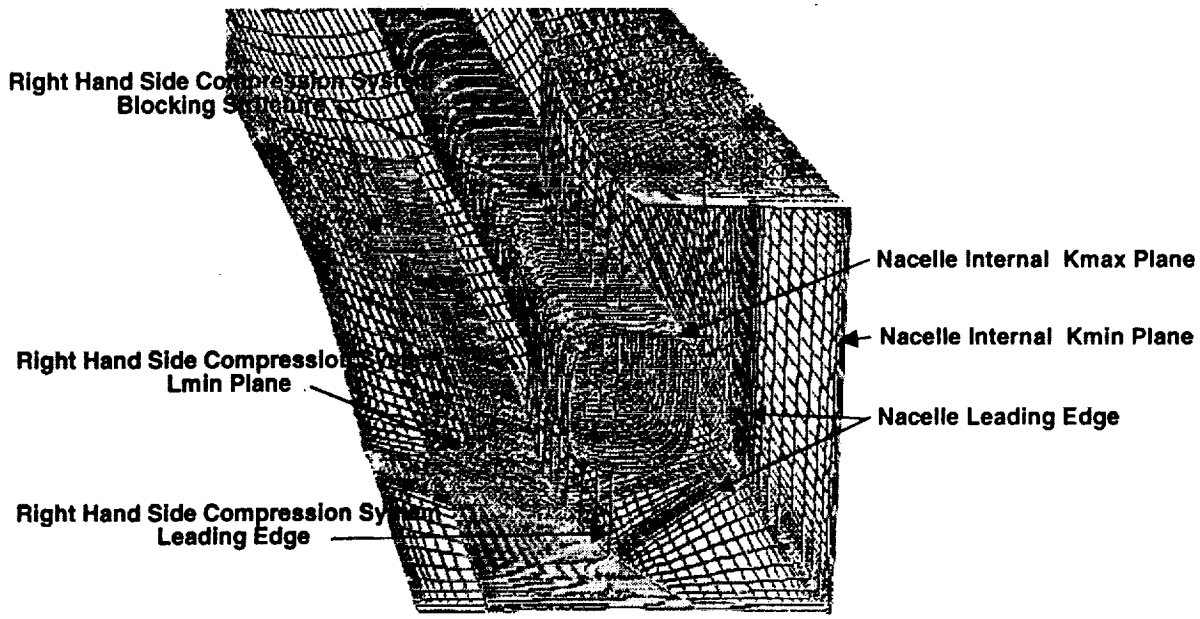

CFD Model(s) Development, BTSSI Compression System Gridding

The BTSSI compression system geometry modeling process adopted a preferred topology and blocking strategy. The fall-back approach to the grid topology selected was selected when difficulties arose while PEGSUS was being exercised in defining the overlap interpolators. In order to capture the viscous interaction between the ramps and inlet sidewalls, a block H-H grid topology was selected. Each nacelle has two additional blocks that share the geometry of the internal nacelle and ramps. The blocks overlap for approximately 50% of their length on both the leading and trailing edges of the ramp(s). Each block's dimensions were 109 x 75 x 45.

The BTSSI nacelles/compression system grids required several modifications that enabled PEGSUS to formulate high quality (orphan-free) interpolators. Our efforts entailed preservation of the existing grid topologies from the flow-through cases (examined in earlier studies) and adapting collar grids which were used to tie the ramp-to-wall regions together. For illustration purposes the H-H ramp blocks, H-O nacelle internal block and O-H ramp collar grid are shown in figure. Complete geometry representations which required the internal collar grids were:

isolated BTSSI without compression system,
isolated BTSSI with 1st ramp and Mach 1.3 outflow plane,
isolated BTSSI with 1st ramp,
integrated Ref. H/BTSSI with 1st ramps and Mach 1.3 outflow planes,
integrated Ref. H/BTSSI with 1st ramps.

The completed grids were used for subsequent OVERFLOW analysis and comparison with experimental data.

REF H WITH MCTCB NACELLES / CENTERBODIES IN PROXIMITY AT MACH 1.80

HSCT High Speed Aerodynamics

Aerodynamic/Propulsion Reference Conditions
Extrapolated Outflow Boundary Conditions Prescribed for Inlet
Freestream Inflow Boundary Conditions Prescribed for Nozzle

Wing/Body/Nacelle Interference Effects
Centerbodies and Cowl Surface Cp's at AOA= 4.4 Degrees
OVERFLOW CFD Results
Viscous Solution using Chimera Grid Strategy
Re 3.0 Million/ft.

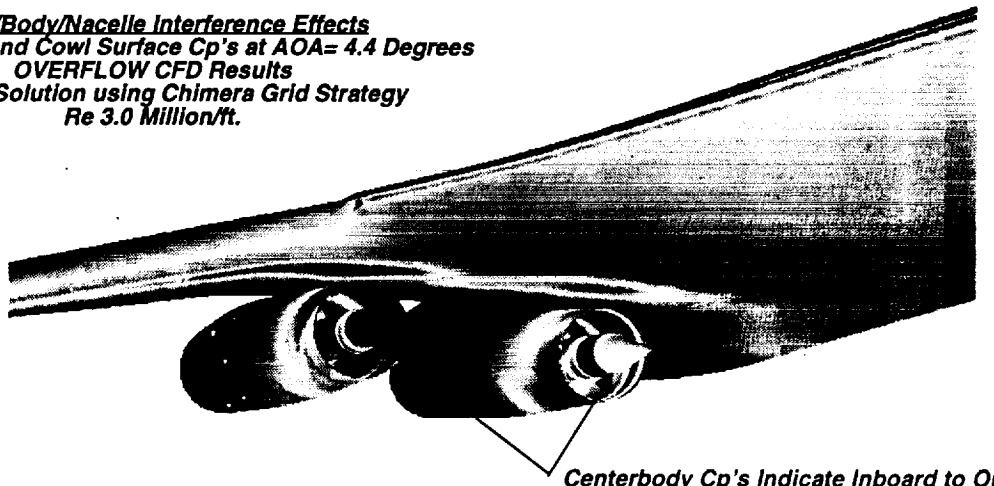

Centerbody Cp's Indicate Inboard to Outboard Mach Number Variation

PRESSURE COEFFICIENT

-0.40 0.05 0.50

OVERFLOW Surface Pressure Results for Reference H / MCTCB

The behavior of the inboard and outboard MCTCB nacelles and centerbodies is shown in figure with respect to the static pressure coefficient values at a freestream Mach of 1.80. The regions internal to each of the nacelles show somewhat differing in magnitude. To insure that the internal shock losses did not affect the nacelle external flow and nozzle performance and in-turn deviate from the flow-through aerodynamics reference condition, the CFD boundary conditions were selected and set for both the inlet and the nozzle of each nacelle. The inlet outflow was extrapolated at the mid-nacelle location, while freestream inflow conditions were set internal to the nacelle midpoint. Points stranded between the inflow-outflow bounds were simply removed from the computations using the IBLANK option.

REF H WITH BTSSI NACELLES / RAMPS IN PROXIMITY AT MACH 1.80

Aerodynamic/Propulsion Reference Conditions
Extrapolated Outflow Boundary Conditions Prescribed for Inlet
Freestream Inflow Boundary Conditions Prescribed for Nozzle

Wing/Body/Nacelle Interference Effects
Ramp and Cowl Surface Cp's at AOA= 4.4 Degrees
OVERFLOW CFD Results
Viscous Solution using Chimera Grid Strategy
Re 3.0 Million/ft.

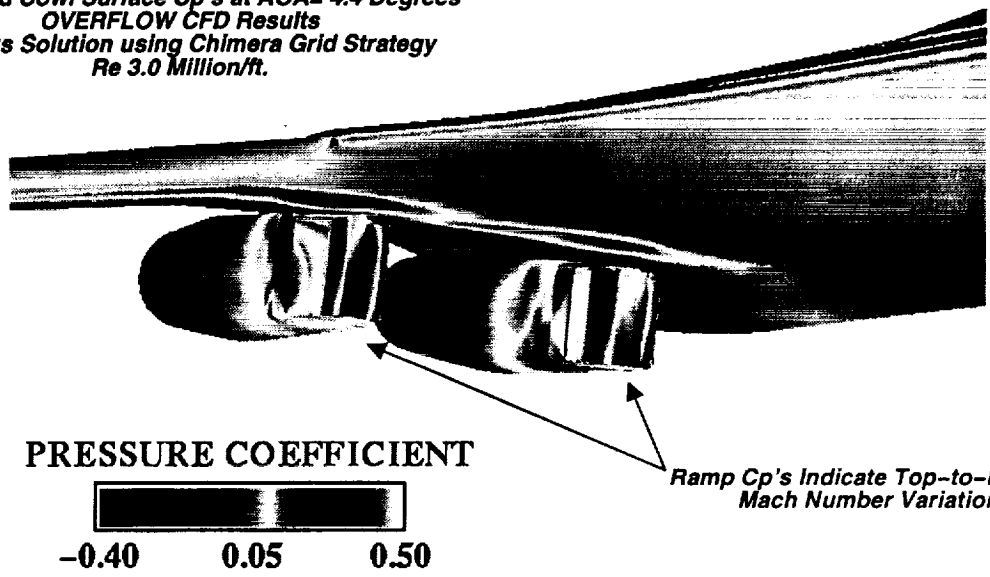

OVERFLOW Surface Pressure Results for Reference H / BTSSI

Static pressures on the nacelles and inlet ramps are shown in figure above. Ramp and cowl pressure again indicate a small amount of Mach number variation in the capture flow for each nacelle. The boundary conditions were set to insure that the aerodynamic reference conditions replicated the test as much as possible.

OVERFLOW Computations at Mach 1.80

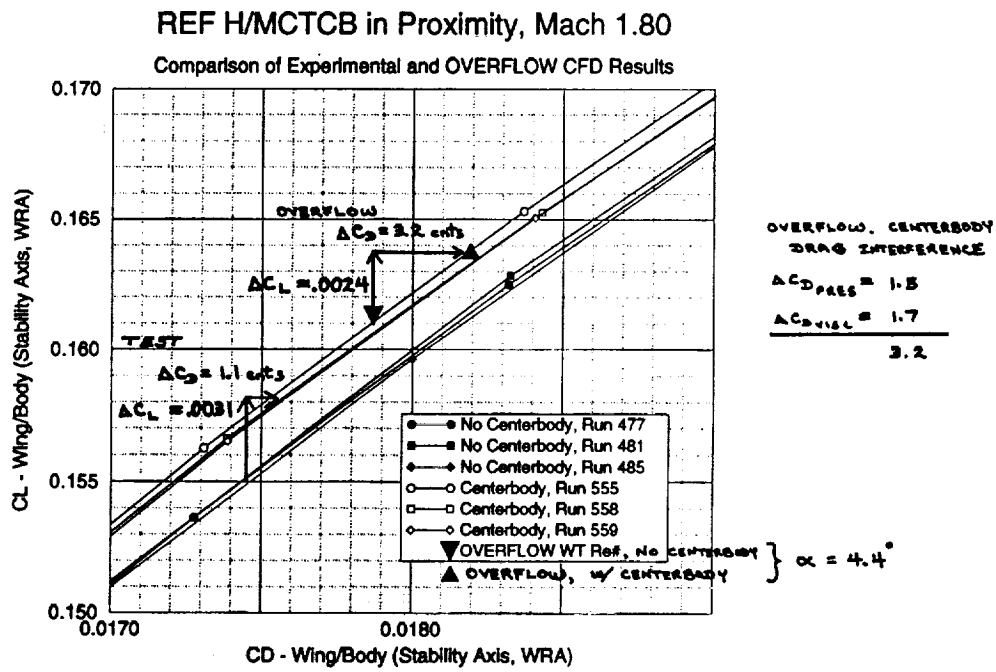

The test data indicates a favorable wing/body interference due to centerbody at Mach 1.8 of -2.2 counts at constant lift. The OVERFLOW result for the no centerbody case with axisymmetric flow through nacelles-in-proximity is very similar to the OVERFLOW results at Mach 2.4, about 2 to 3 counts less than the test data. The OVERFLOW prediction of the centerbody supersonic spillage effect obtained the correct trends but the absolute magnitude is off. The test data indicated a lift increment of 0.0031 at constant angle of attack, OVERFLOW predicted 0.0024. The OVERFLOW drag increment was substantially higher than test increment at constant angle of attack. Half of the OVERFLOW drag increment was due to changed friction drag on wing.

OVERFLOW Computations at Mach 1.80

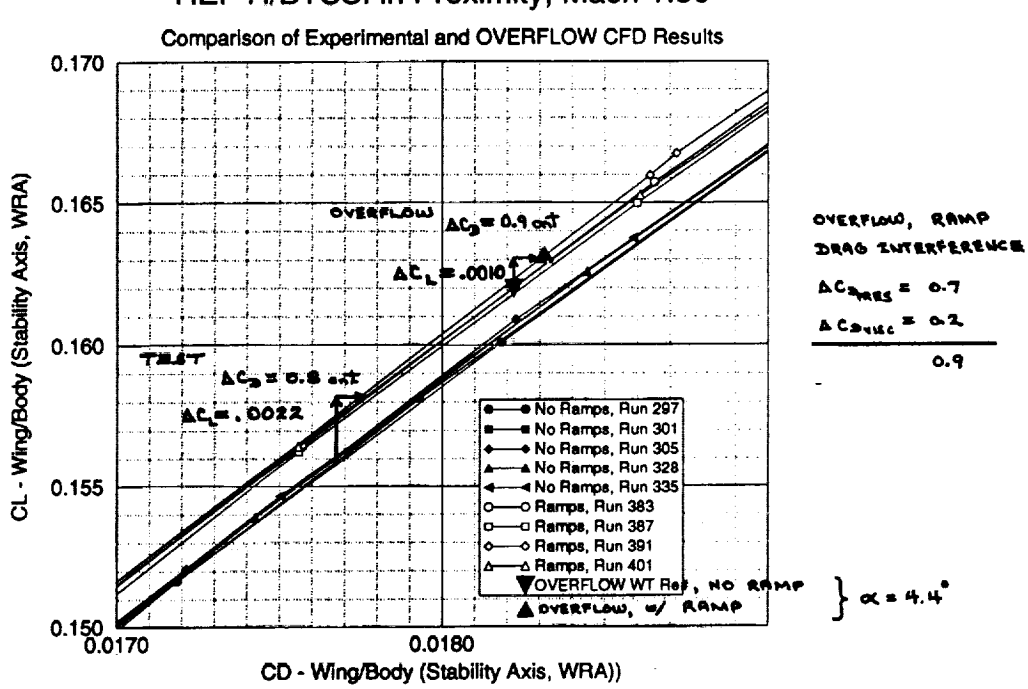

The test data indicates a favorable wing/body interference due to ramp at Mach 1.8 of -1.5 counts at constant lift. The OVERFLOW result for the no centerbody case with axisymmetric flow through nacelles-in-proximity is very similar to the OVERFLOW results at Mach 2.4, about 2 counts less than the test data. The OVERFLOW prediction of the centerbody supersonic spillage effect obtained the correct trends but the absolute magnitude is off. The test data indicated a lift increment of 0.0022 at constant angle of attack, OVERFLOW predicted 0.0010. The OVERFLOW drag increment was nearly equal to the test increment at constant angle of attack.

The spillage interference due to the bifurcated inlet compression ramp is measurably less than the axisymmetric centerbody interference. This is not surprising as the bifurcated pushes most of the spillage flow to the sides of the inlet, while the axisymmetric has large component of spillage redirected up into the wing lower surface.

Conclusions and Recommendations

- **Much more to learn from Ames spillage data.**

- **Wing/body spillage interference is small and favorable:**
  - **Axi / Centerbody interference = -2.2 cnts (M=1.8),**
  - **Bif / Ramp interference = -1.5 cnts.**

- **CFD captures trends and magnitudes.**
  - **More analysis required to improve absolute accuracy.**

Conclusions and Recommendations

Data acquired in the NASA-Ames Reference H / NAI Tests are of high quality and represents the state-of-the-art in nacelle-airframe interference databases. Future use of the database should include a detailed tare bookkeeping reassessment with respect to the nacelle flow-through balances. Small differences in projected areas within the balance may result in additional corrections and potentially decrease the differences between experiment and analytical models

Nominal spillage effects are small and to be determined accurately using CFD requires that the pressure gradient effects on the wing/body's lower surface be modelled accurately in the analysis. Future work should include grid convergence sensitivity studies for the nacelles in proximity using spacings which are compatible with the nacelle's near wall spacing.

SUPERSONIC CRUISE PAI STUDIES

Team Members: Steve Chaney - Aerodynamics
Steve McMahon - Propulsion
Steve Ogg - Aerodynamics

This section contains all the supercruise studies performed by Boeing. Steve Chaney and Steve Ogg are members of the Boeing HSCT High Speed Aerodynamics staff. Steve McMahon is a member of the Boeing HSCT Propulsion Design staff.

CONFIGURATION DEFINITION

- Reference H Configuration
  - Baseline Nacelles: Axi Inlet, Axi Nozzle, 509 pps
  - Bifurcated : Bifurcated Inlet, Axi Nozzle, 509 pps
    * Nozzle has slight variation from baseline.
- Nacelle Installations Configured this year:
  - DSM Nozzle: Axi Inlet, 2-D nozzle, 673 pps (Supersonic & Transonic Nozzle settings)
  - Axisymmetric Equivalent of DSM: Axi Inlet, Axi Nozzle, 673 pps (Supersonic & Transonic Nozzle settings)
  - Bifurcated/DSM: Bifurcated Inlet, 2-D Nozzle, 673 pps
    * Straight inlet dropped to provide outboard channel clearance,
    * Reflexed inlet to provide clearance.
  - Axi Inlet, DSM Nozzle, 509 pps
  - Bifurcated Inlet, DSM Nozzle, 509 pps

The wing/body used for these studies was the Ref. H. The baseline nacelles designed for this configuration had axisymmetric inlets / axisymmetric nozzles, and flowed 509 pps. A bifurcated inlet / axisymmetric inlet nozzle nacelle was designed for the ARC testing of the 2.7%-scale Reference H. Since the Reference H configuration was developed the engine size required for a given wing size has grown. A nacelle was configured that represented the current 'best' design for the Ref. H wing. The result was a nacelle that flowed 673 pps, had an axisymmetric inlet, and a 2-D nozzle. Nozzle settings were configured for this nacelle for both the supersonic cruise condition and transonic conditions. In order to assess the 2-D nozzle versus axisymmetric nozzle effects on airplane aerodynamic performance an axisymmetric equivalent of the 2-D nozzle was designed and attached to the same inlet. An installation of a bifurcated inlet nacelle with the 2-D DSM nozzle on the Ref. H was also performed. The axi - 2D and bifurcated - 2D nacelles were also scaled down to 509 pps and installed on Ref. H to enable comparisons to the original Ref. H baseline nacelles.

The installation guidelines were: (1) diverter LE height equal to boundary height at nacelle inlet, (2) nacelles not buried in wing, (3) nacelle maximum diameter (break between forecowl and nozzle boattail) located as close as possible to wing TE. In addition, the diverter was constrained by a structural box width that the inlet attached to; resulting diverter width was 32 inches. Diverter LE was located 6 inches back from inlet lip.

It was possible to locate the 673 pps axisymmetric inlet - DSM nozzle nacelles using these guidelines, however, as one of the following figures discusses, this installation had a wing/diverter/nacelle channel at the wing TE that was considered too small. The nacelle maximum diameter was moved down (while holding diverter LE height constant) to alleviated this channeling. Both the 509 and the 673 bifurcated inlet nacelles were too long to install and adhere to all of the above the rules. The 509 bifurcated nacelles were installed with the same TE diverter height but the diverter LE height was nearly twice as big as required. The 673 bifurcated required dropping both the inlet and the nacelle maximum diameter down to prevent burying nacelle in wing and choking the diverter channel completely. A 673 bifurcated installation was also completed with a reflexed (curved) inlet shape to nearly meet meet all the guidelines above.

Baseline Nacelle Configurations
509 pps

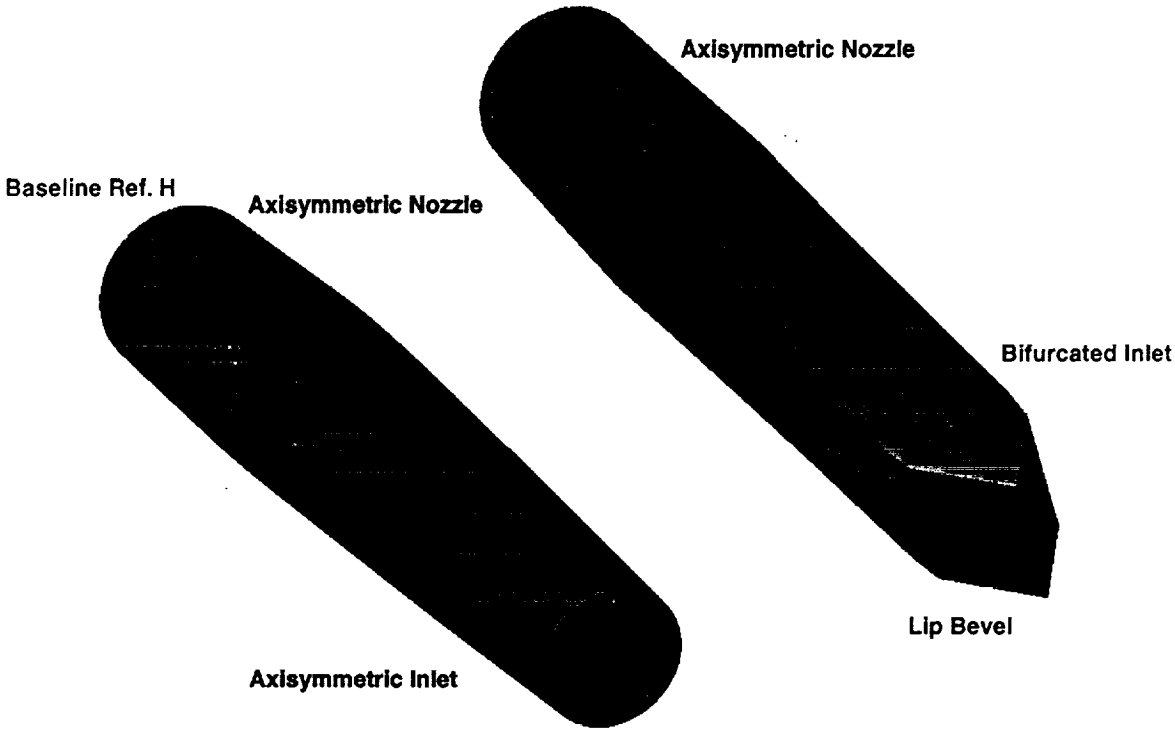

The two baseline Ref. H nozzles as tested in the ARC 2.7%-scale model tests are shown. The key difference between the two was the square cross section of the bifurcated inlet and the bifurcated lip bevel necessary for structural rigidity. The nozzles were only slightly dissimilar and were assumed to be the same aerodynamically. However, detailed analysis of PAI aerodynamics in this study showed that the 'slight difference' was definitely measurable and had a significant effect on results. The axi-axi nacelle had a slightly longer and canted downward nozzle that carried more lift than the bifurcated nacelle nozzle. This will be discussed in more detail in later charts.

DSM INSTALLATION ON REFERENCE H

673 pps / 7100 sq.ft.

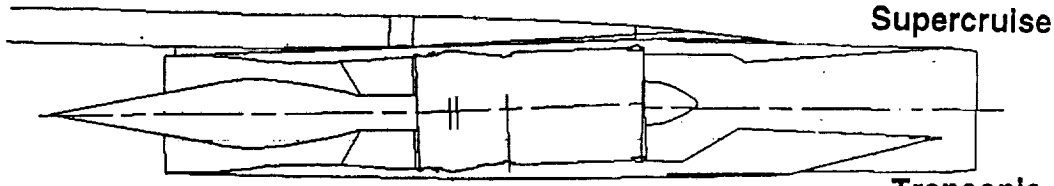

Axisymmetric Inlet / 2-D Nozzle

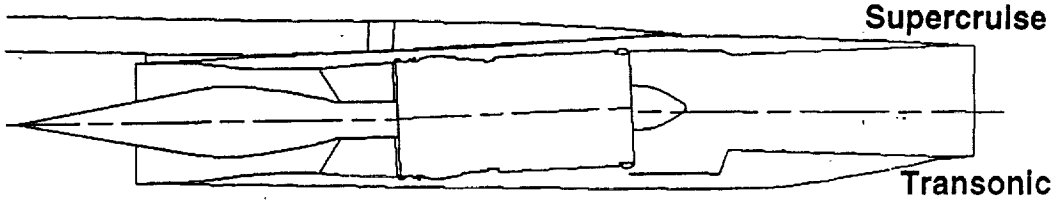

Axisymmetric Inlet / Axisymmetric Equivalent Nozzle

Cross-Section @ Wing TE

The installation of the DownStream Mixer (DSM) nozzle on the Ref. H wing is shown for both the baseline 2-D nozzle and the axisymmetric equivalent. The current design guideline for axisymmetric nacelles of locating the maximum diameter at the wing TE had to be modified for the 2-D nozzle if the same diverter is kept. As shown, the nacelle was dropped down to alleviate any choking that might have occured in the channel between the wing, nacelle, and diverter. The diverters for the two configurations were kept the same in order to provide as consistent a comparison between the them as possible.

Alternative diverter designs were investigated that extend to the full width of the nacelle to completely remove possibility of choking in channel and could allow moving 2-D nozzle back up to wing.

Transonic Nozzle Study Configurations

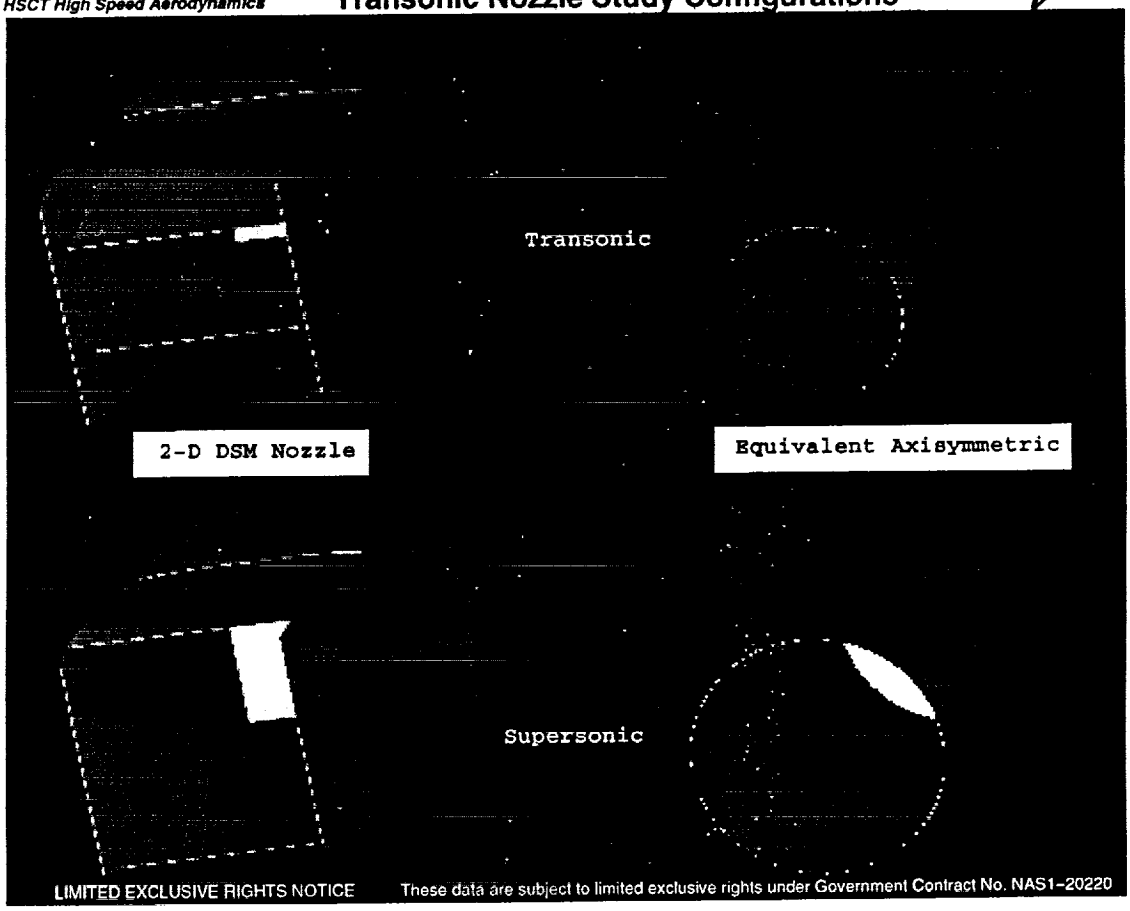

Details of the 2-D and axisymmetric nozzles at the supersonic and transonic operating conditions are shown. The key feature of the 2-D nozzle at the transonic condition was the side walls or 'ears' on either side of the nozzle. Another important feature was the large nozzle angles at the transonic conditions for both the axisymmetric and 2-D that lead to separation of the external flow.

ANALYSIS / DESIGN TOOLS

- Linear Theory - Current PD tool.
  - Linear B.C. means axisymmetric nacelles, no diverters.
- TRANAIR (Full Potential) - W/B optimization, PAI analysis
  * Solution adaptive.
  - Most versatile higher order method.
- OVERFLOW (N-S) - W/B, W/B/N detailed analysis.
  * Central difference, ARC3D.
  * Baldwin-Barth.
  - Most accurate method.

The current PD tool for HSCT PAI design and analysis is the linear theory design code. The studies in this task were all performed with TRANAIR and OVERFLOW due to the complex geometry modeling required and the requirement to assess viscous effects.

TRANAIR is a Boeing developed code for analyzing compressible flow over arbitrary complex configurations at subsonic, transonic, or supersonic freestream Mach numbers. It solves the non-linear, full potential equation subject to a variety of boundary conditions, modeling wakes, inlets, exhausts, porous walls, and impermeable surfaces. The flow field is divided into a locally refined rectangular grid which is generated internally by the code. This grid may be adapted to the solution through a sequence of several grids. The surface boundary is divided into networks of panels where separate boundary conditions can be specified. TRANAIR is usually executed on a CRAY for typical wing/body/nacelle configurations.

OVERFLOW, a thin layer Navier-Stokes code using overset grid methodology, was developed at NASA Ames. In this multi-block method the individual grids are not required to match exactly at boundaries, but instead must overlap in order for information to be passed from one grid to another. The Baldwin-Barth turbulence model was used for nearly all viscous runs made for this study. All the OVERFLOW runs were done on the NAS C-90.

ANALYSIS TOOL FLOW AND SOLUTION TIMES

Code	PreProcessing, Gridding,etc	NAS Solution C90 hrs	NAS Solution Clock hrs
Wing / Body			
Linear Theory	< 1/2 day	–	–
TRANAIR 500k boxes	1/2 - 2 days	2.5 hrs	6 - 16 hrs
OVERFLOW 2.9 million pts	1 - 5 days	7 hrs	6 - 16 hrs
Wing / Body / Nac / Diverter			
Linear Theory	< 1/2 day	–	–
TRANAIR 750k boxes	1 - 10 days	3 hrs	6 - 16 hrs
OVERFLOW 7-8 million pts	2 - 30 days	15 - 20 hrs	overnight

As a result of continuing pressures on NAS computer resources, and discussions that occured at the HSR CFD workshop in February of this year, an effort was made to reduce the size of the OVERFLOW grid as all of the different PAI configurations to be analyzed were to be built on this grid. In addition, some refinements were made to improve the force prediction accuracy (see following chart).

The OVERFLOW grid sizes and solution times (as charged on NAS C-90) are shown below, along with similar data for TRANAIR, and typical pre-processing flow times. Both the TRANAIR and OVERFLOW gridding flow times are highly dependent on the similarity of the new loft with the previous loft gridded, the format of the loft's surfaces, and whether a new grid topology is required.

OVERFLOW GRIDDING / DRAG STUDIES

- OVERFLOW Grid Size Reduced Considerably
  - * No Loss In Accuracy (Wing/Body: 4.5 million to 2.9 million).
- Detailed Absolute Drag Analysis Lead to Process Changes:
  - * OVERFLOW Force Integrator (FOMOCO) With Specified Temp.
  - * Three cells of constant size at wall before stretching radially.
- Detailed comparison of OVERFLOW and test results highlighted uncertainties in test data that need to be resolved:
  - * Trip Drag
  - * Aeroelastic Effects
  - * Internal Nacelle Duct Forces

The OVERFLOW gridding process was improved throughout the year to both improve efficiency and improve accuracy. The surface grid density was changed only slightly. The fuselage grid was refined somewhat at the tip and tail, and grid stations were added to match wind tunnel aft body cut-off stations exactly for force integrations. This was a very dense surface grid, especially around the nacelles. The distance to the first point off the surface in the volume grid to yplus=1 for the ARC 9x7 test condition. The length of the wing C-grid aft of the TE was decreased from 2000 inches to 400 inches. The amount of overlap between several of the grids was more than required; it was decreased. The box grid around the wing/body had extended to the outer boundary. The box grid was reduced in size to just enclose the wing/body, and an ellipsoidal grid was then extended to the outer boundary. The wing C-grid was spread vertically aft of the TE to improve communication with adjacent grids. The grid was changed to have three equally spaced cells at the surface.

Detailed comparison of the OVERFLOW results with test data indicated that the CFD results were very accurate, but there were some unresolved uncertainties that cloud the final conclusions to some degree. These uncertainties are the drag of the boundary layer trip disks used in the AMES 9x7 tunnel, the change in the wind tunnel measured forces due the the aeroelastic deflection of the wing, and the internal nacelle duct lift pressure force which turned out to be not insignificant as has been assumed; each is discussed in following charts.

Ref. H Wing/Body/Nacelle/Diverter OVERFLOW Surface Grid Inboard Axisymmetric and Bifurcated Inlet Installations

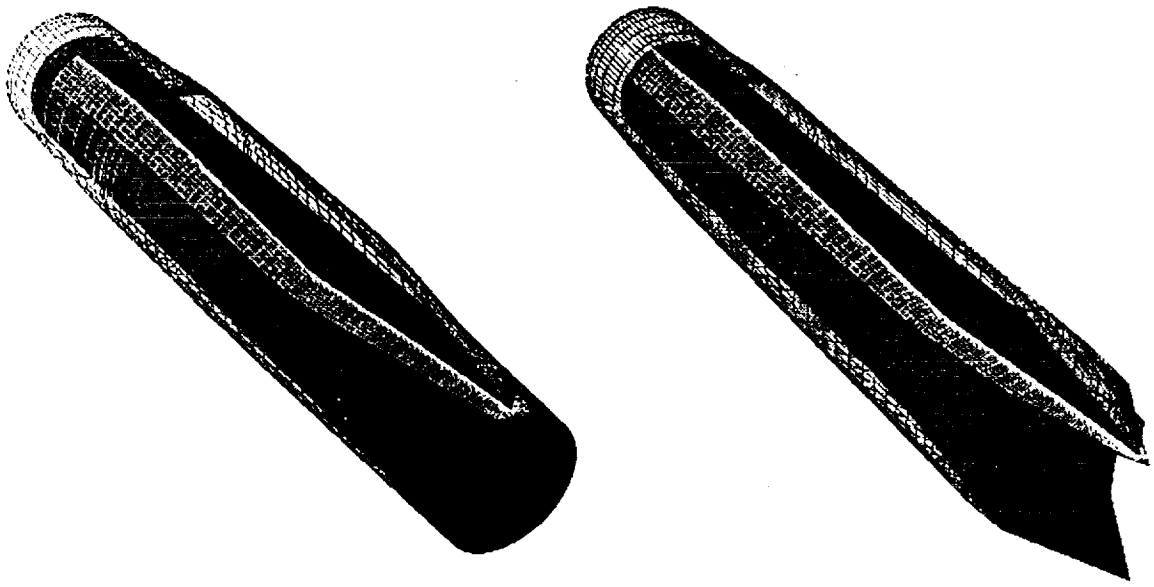

Grid points have been removed for clarity.

The OVERFLOW grid for the wing/body/nacelle/diverter configurations used 17 blocks; 5 for the wing/body, and 3 each for the nacelles, and 2 for each diverter. The bifurcated inlet nacelle has 8.3 million grid points, the axisymmetric had 7 million. This grid has a very dense surface distribution around the nacelle installation. The volume distribution has been built for the NASA Ames 9x7 test condition with the 2.2%-scale Ref. H model.

The nacelle and diverter surface grids are shown in the figure (for the inboard nacelles). The diverter sides were modelled with a single grid that wraps around the LE of the diverter. The diverter aft fairing was a separate grid that overlaps onto the wing upper surface and the nozzle. The nacelle was made up of 3 grids: forecowl, nozzle, internal.

A polar was run for both inlet types to allow a complete comparison of aerodynamic characteristics. Each angle of attack was typically run 1600 to 2000 steps from scratch (no restarts) and cost 15 to 20 hours on vonneumann. After 1600 steps the residuals were converged 3 orders of magnitude or more for every block.

Ref. H Wing/Body/Nacelle/Diverter Lower Surface Pressure Contours Axisymmetric Inlet – Axisymmetric Nozzle, Mach 2.4, α = 4.4, Re_{MAC} = 7 million

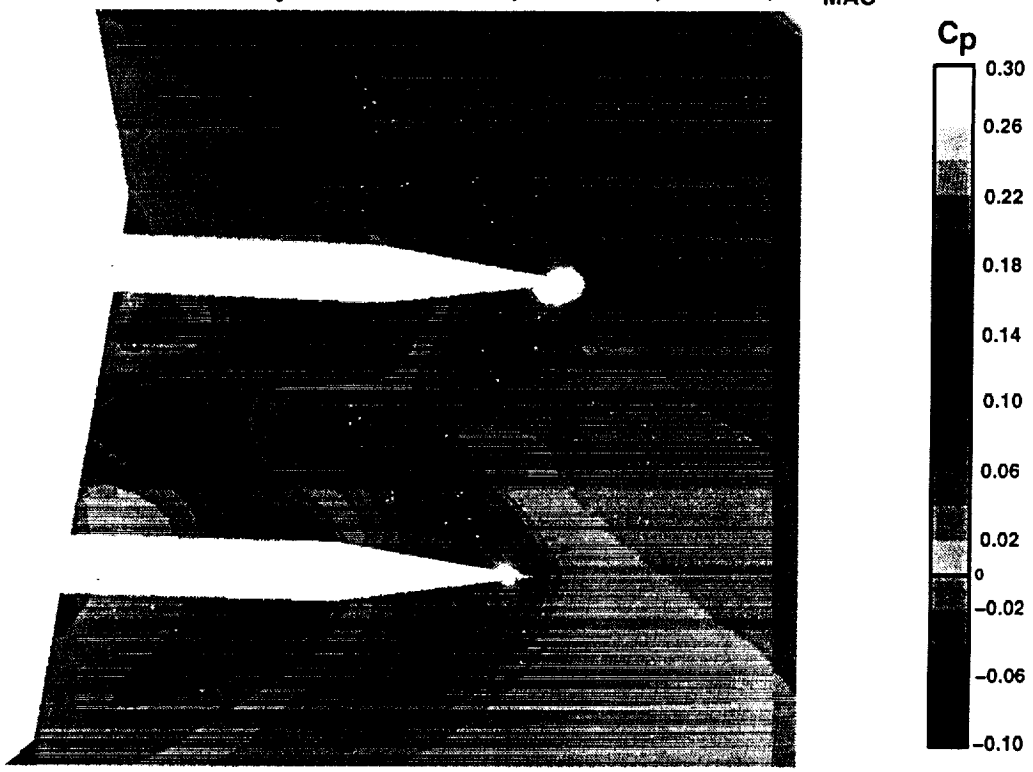

The wing lower surface pressure contours from OVERFLOW are shown in the figure for the captive axisymmetric configuration (wing/body/axisymmetric/diverter). The diverter planform can be clearly seen. The pattern was a typical one seen previously in TRANAIR simulations of nacelle installations: diverter shock merging with nacelle shock, expansion at diverter shoulder, recompression along diverter sides (and some influence from adjacent nacelle). The primary difference from TRANAIR surface pressure contours for the same case was the shock angle from the diverter being more swept forward for the OVERFLOW solution due to diverter buried in boundary layer (TRANAIR pressure contours for this same case are shown later in the diverter study section).

Ref. H Wing/Body/Nacelle/Diverter Lower Surface Pressure Contours
Bifurcated Inlet – Axisymmetric Nozzle, Mach 2.4, α = 4.4, Re_{MAC} = 7 million

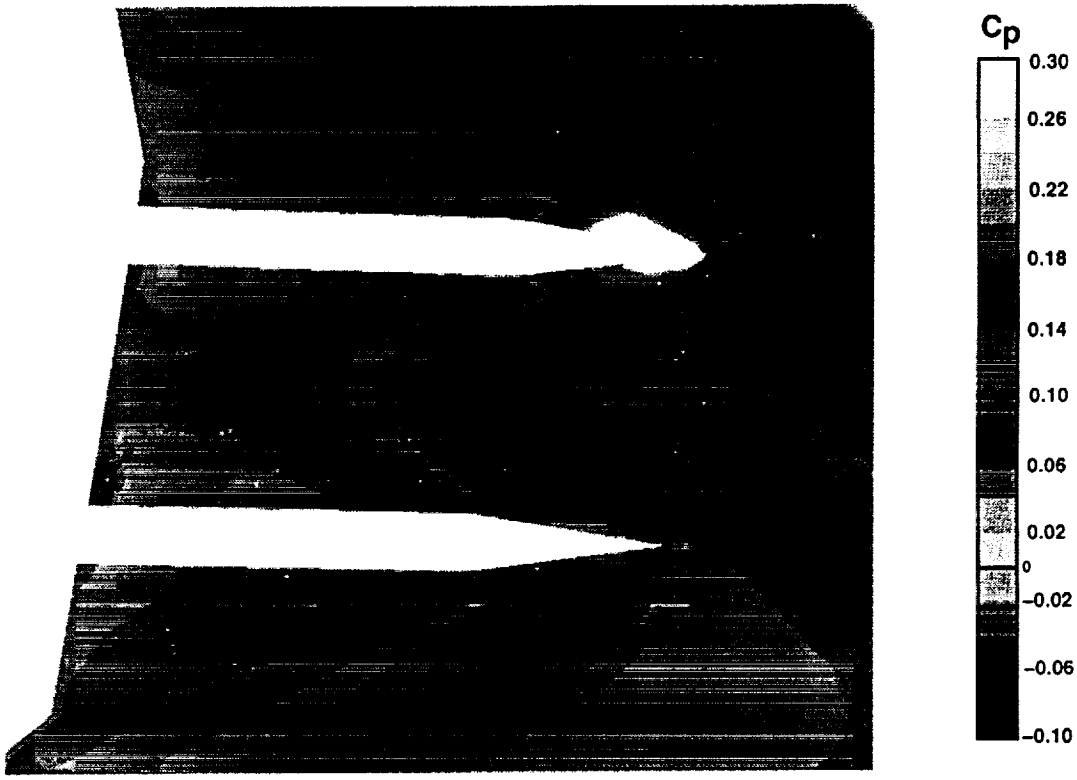

This figure shows the lower surface pressure contours for the bifurcated installation. Comparing with the previous figure some appreciable differences were noted. The additional length of the inlet/diverter pushed the highest pressure region forward on the wing; the low pressure off the diverter shoulder expansion covered a larger area of the wing. The high pressure region near the front of the inlet/diverter was much larger for the bifurcated than for the axisymmetric. This was due to the relatively high angle of the lip bevel on the bifurcated creating a shock and resulting high pressure that raised the pressure on all the surrounding components. Pressure integration on the wing lower surface indicated that the bifurcated configuration had higher total lift on the wing than the axisymmetric (CL = 0.04719 versus 0.04666). Note that these pressures also acted on the nacelle upper surface to create a negative lift force that was amplified in the case of the bifurcated by the flat top of the inlet.

Ref. H Wing/Body/Nacelle/Diverter Lower Surface Oil Flow
Axisymmetric Inlet – Axisymmetric Nozzle, Mach 2.4, α = 4.4, Re_{MAC} = 7 million

The next two figures are identical to the previous two except that the nacelles have been added and surface streamlines (simulated oil flow) have been plotted. The figure below is the axisymmetric installation. The following figure is the bifurcated installation. The streamline patterns are very similar for the two nacelles. The nozzles on the axisymmetric installation were observed to carry slightly more positive pressure on the lower surface than the bifurcated installation. This has been attributed to the small geometry difference between the two that was discussed earlier in the configuration description section. The effect will be confirmed later in report by more negative pressures on top of nozzle of axisymmetric installation and differences in integrated lift.

Ref. H Wing/Body/Nacelle/Diverter Lower Surface Oil Flow
Bifurcated Inlet – Axisymmetric Nozzle, Mach 2.4, α = 4.4, Re_{MAC} = 7 million

See text for previous figure.

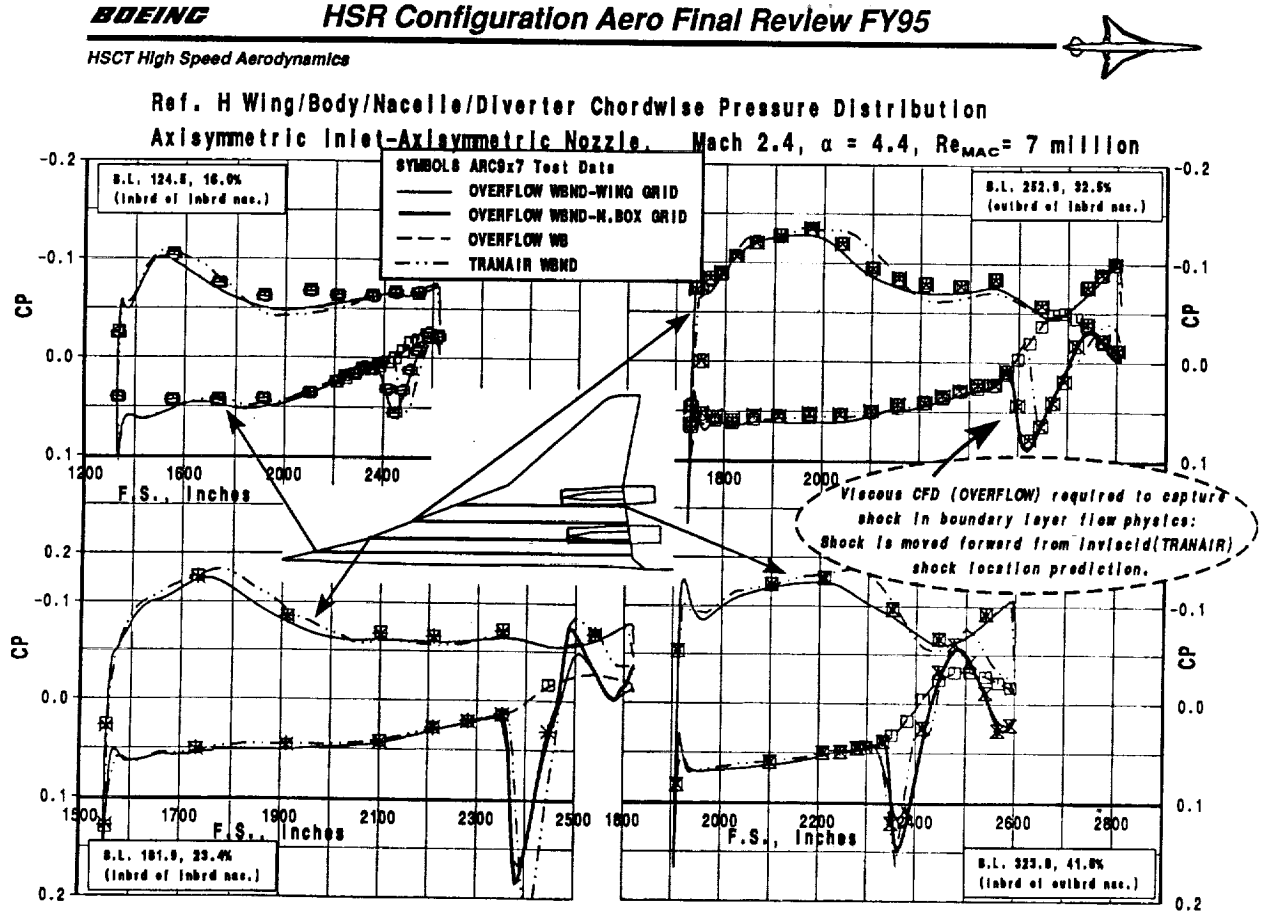

The pressure distribution calculated by OVERFLOW for the captive axisymmetric case is compared with test and TRANAIR in these figures. Chordwise pressure distributions on the inboard wing panel are shown in the figure below. Chordwise pressure distributions on the outboard wing panel are shown following figure. The basic comparison of the theoretical results with the test data for the wing/body upper and lower surface have been discussed extensively previously and will be ignored here; the focus of this discussion will be on the nacelle effects. The results were as expected with the viscous modelling of OVERFLOW providing a consistently better match of the diverter/nacelle shock location on the wing lower surface than the inviscid modelling of TRANAIR. This discrepancy became more pronounced the farther the pressure row was from the diverter. OVERFLOW was able to capture both the location and magnitude of the nacelle/diverter shock very accurately.

One OVERFLOW line was labelled WING GRID; this was pressure data interpolated from the wing grid. The line labelled N.BOX GRID was from the box grid that surrounds each nacelle and also comforms to the wing lower surface. It was slightly more dense than the wing grid as was evident in several of the plots where it captures the steepness of the nacelle/diverter shock slightly better than the wing grid.

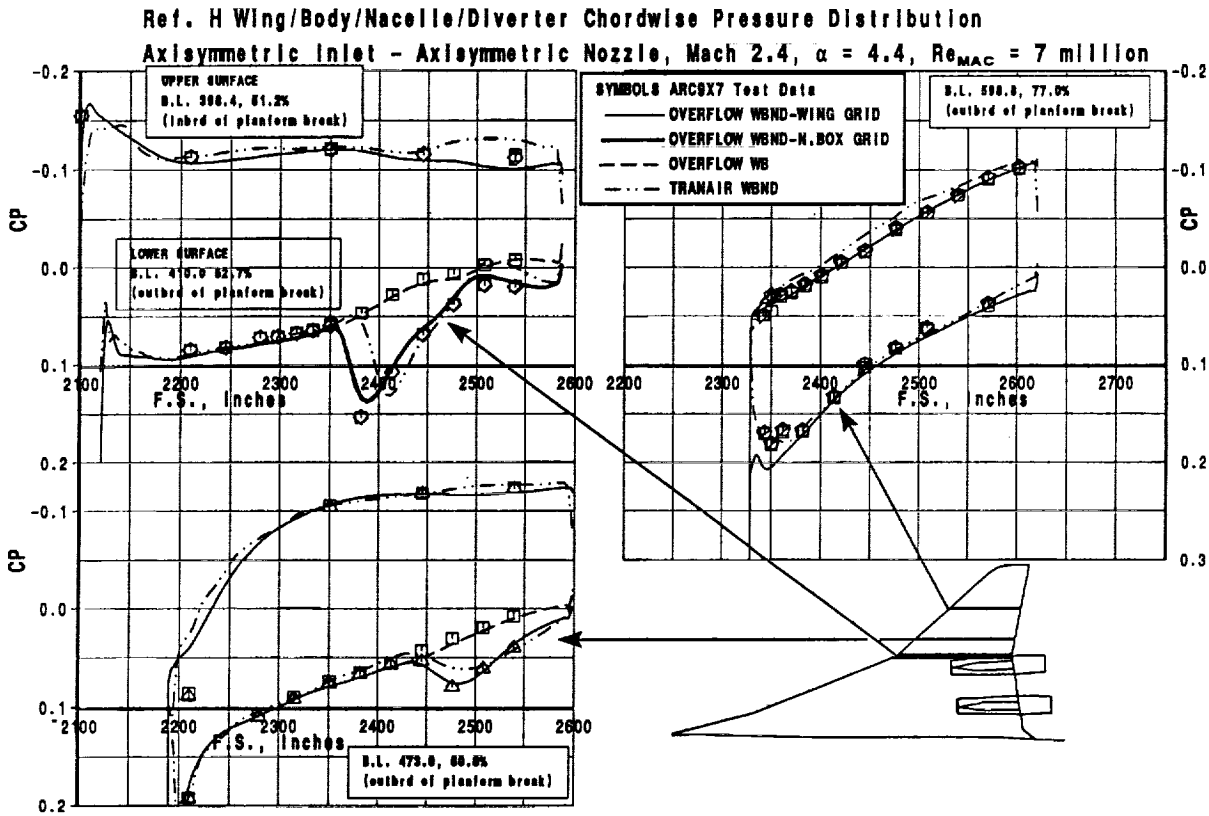

See text for previous figure.

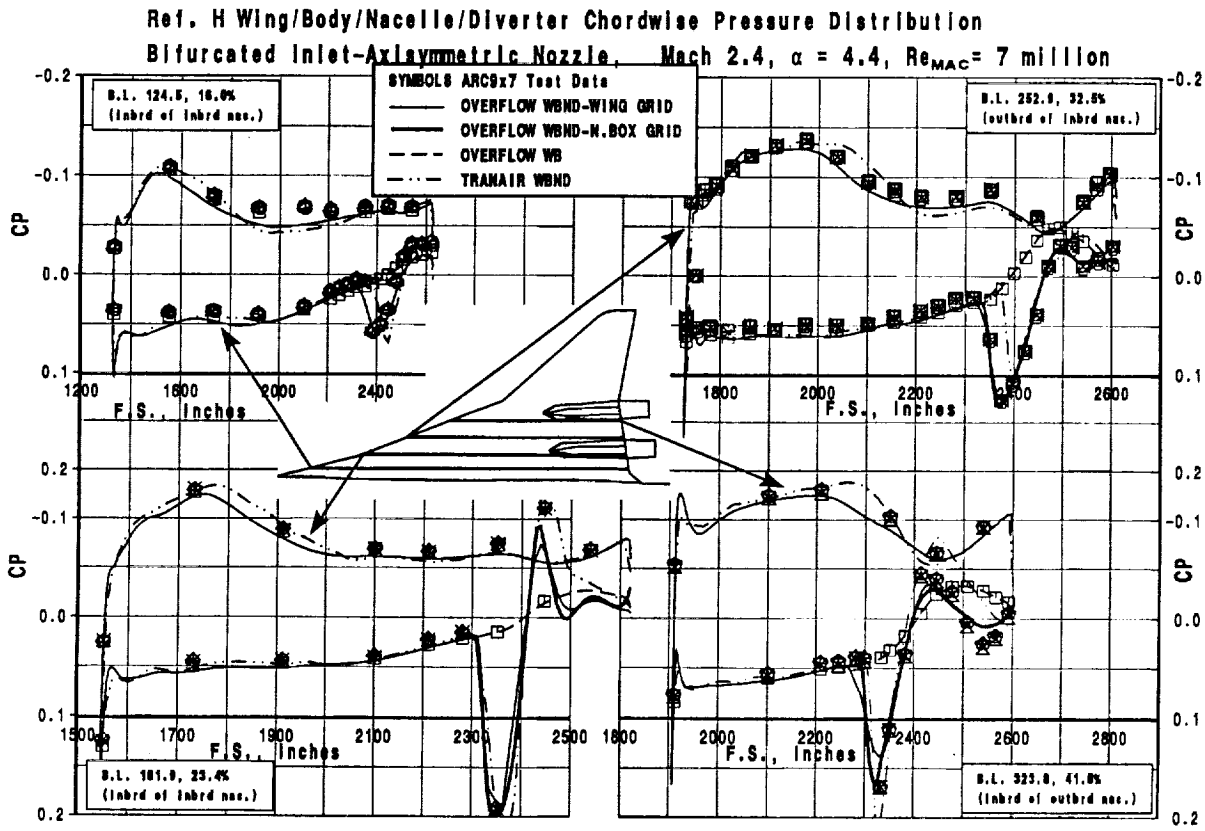

The next two figures are also chordwise pressure distribution comparisons, but for the bifurcated nacelle installation. The shape and magnitude of the nacelle/diverter pressure field was again modelled very accurately by OVERFLOW.

These successful comparisons of OVERFLOW pressure data to the test data lead to the following figures where the pressures have been integrated to produce forces and moments for comparison to test data.

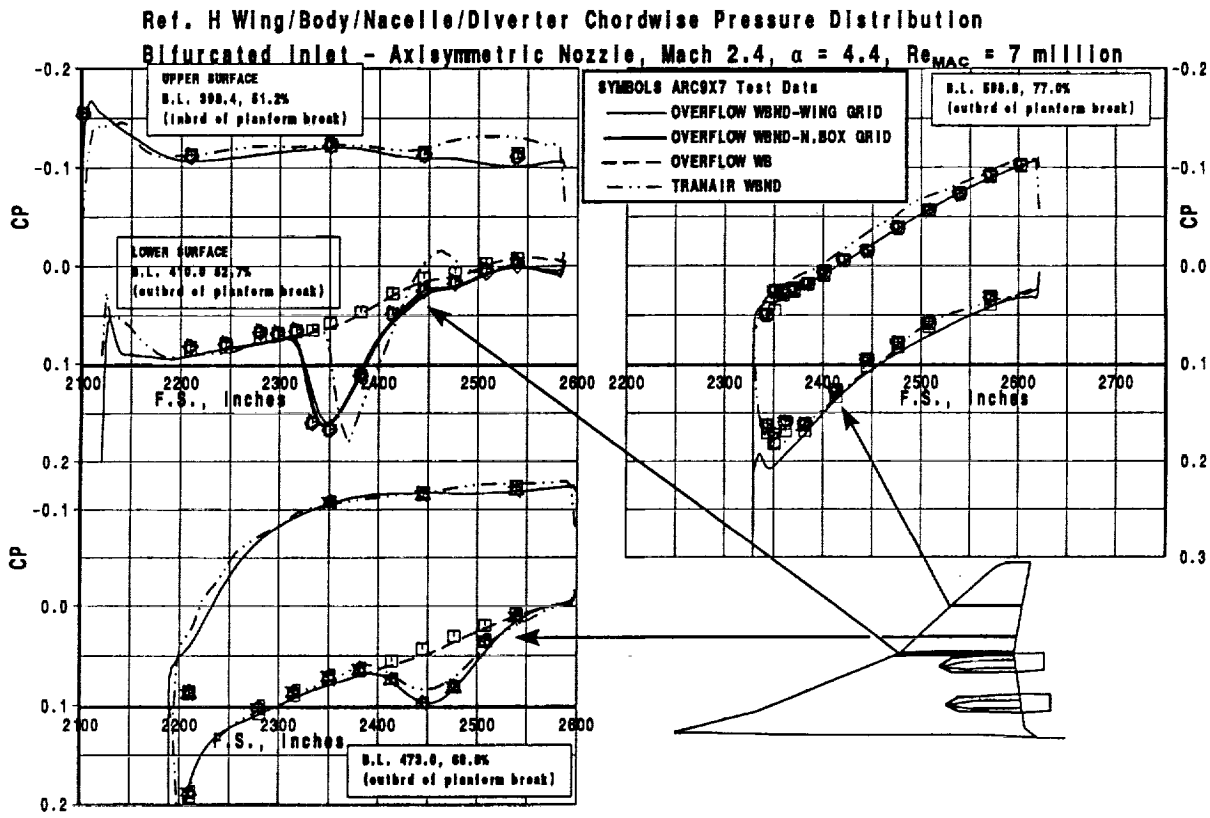

See text for previous figure.

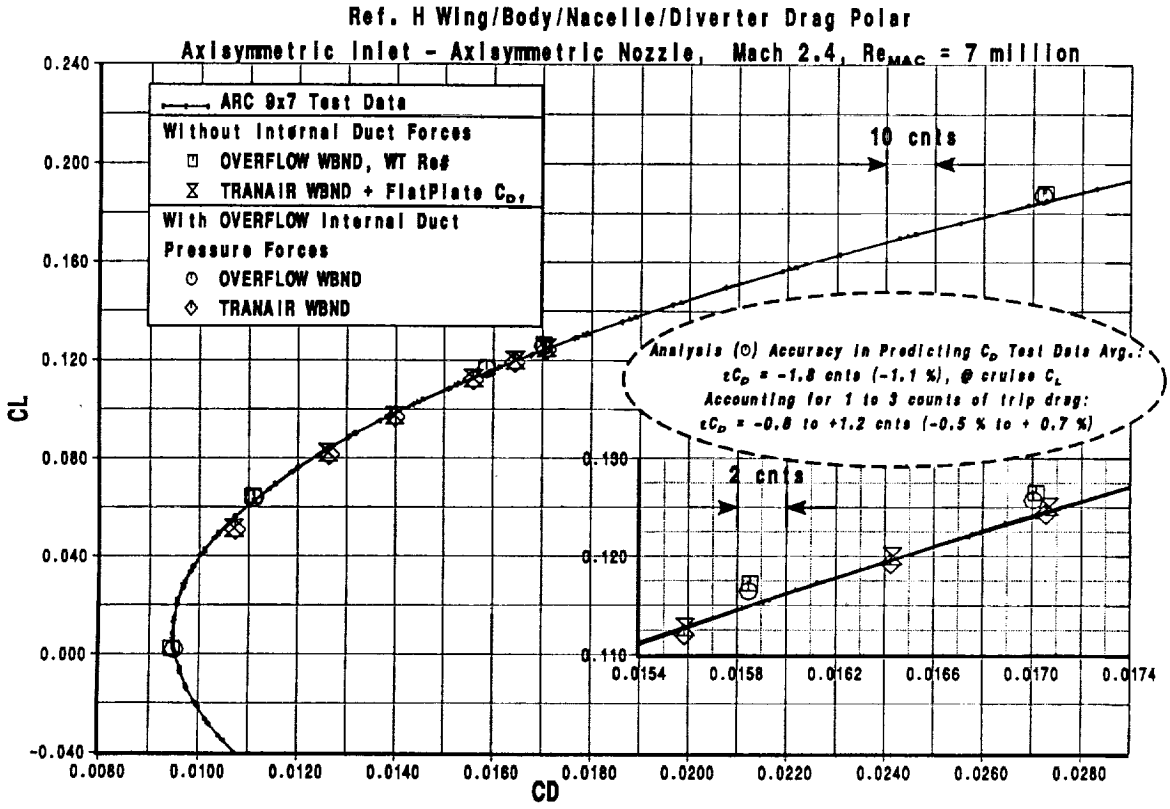

A drag polar for the captive axisymmetric configuration is shown in the figure. The OVERFLOW drag value labelled 'Without Internal Duct Forces' was about 3 counts lower than test. This discrepancy is in-line with previous OVERFLOW solution results for the wing/body and wing/body/nacelle-in-proximity configurations. The discrepancy has been at least partially attributed to the drag of the trip discs which has been found to be 1 to 3 counts. In addition to the trip drag that was in the test data (not corrected out), another discrepancy or correction between test and theory has been discovered. Two corrections were applied to the test data to adjust for unwanted nacelle forces; the base drag was removed and an estimate of the internal skin friction was removed. However, the OVERFLOW results indicated that the nacelle internal ducts were also carrying a large amount of lift (lift coefficient about -0.0013 at cruise, 1% of cruise lift). This value was large enough that it effected the drag polar comparison on the blown-up scales. There are two ways it could be applied, either the OVERFLOW value could be reduced by this amount (the OVERFLOW force integration does not currently include this lift), or the test data could be increased by this value. It was decided to include the internal pressure lift in the CFD data just for the purpose of comparison to the test data. This corrected point was shown as the circle symbol in the figure; it was about 1.8 counts less than the test data drag level at cruise (the OVERFLOW internal duct pressure lift was also applied to the TRANAIR data).

The note surrounded by the dashed oval was added to this plot for the milestone 10 input which required an assessment of CFD accuracy in calculating test data. In this plot, and all other plots that follow that have similar notes the CFD data have been compared to an average of the test data. For the OVERFLOW data shown here, given a trip drag range of 1 to 3 counts, the error was -0.5% to +0.7% of cruise drag.

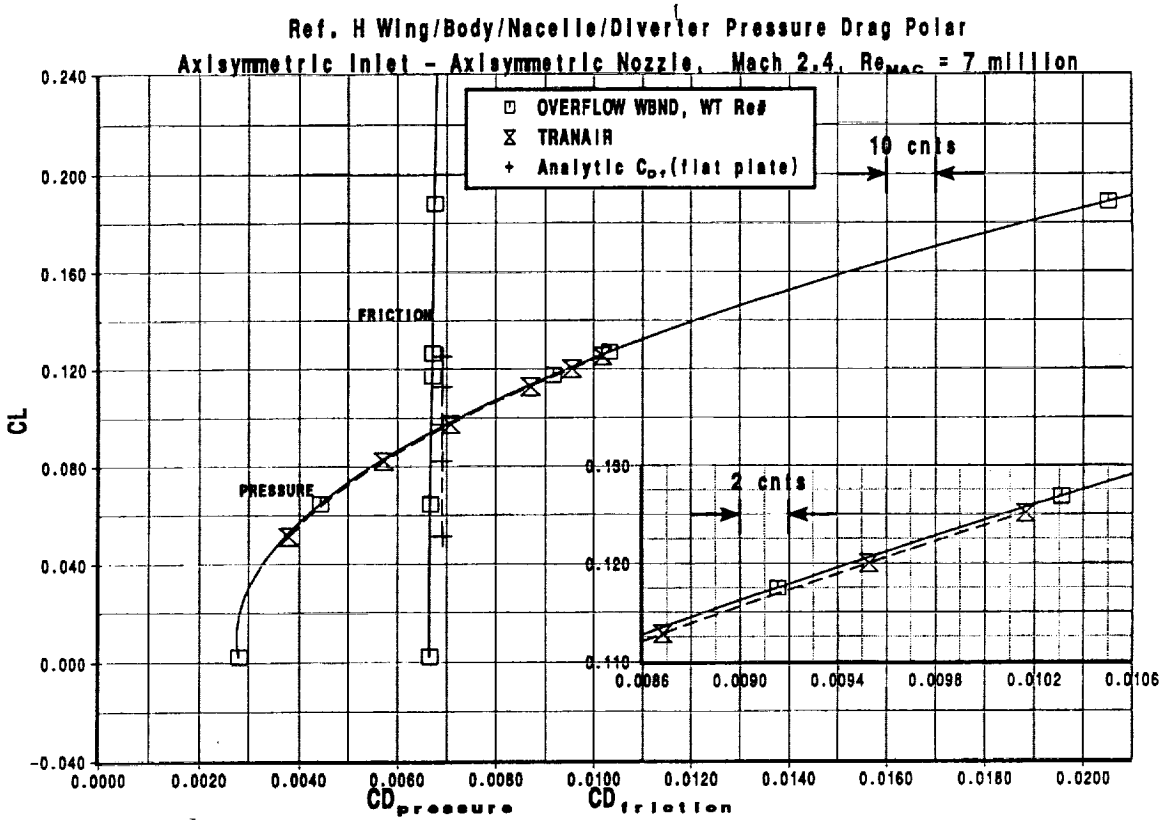

In order to remove friction drag differences between flat plate and OVERFLOW from the OVERFLOW to TRANAIR comparison a pressure drag polar was also constructed. The pressure drag and the friction drag are both shown on the large scale axes. The blown-up axes plot shows that the pressure drag difference between TRANAIR and OVERFLOW was about 0.8 counts at constant lift. Note that although the flat plate and OVERFLOW skin friction values differ by about 2 counts, the assumption of small variation with angle of attack was validated by the OVERFLOW results. The drag difference between OVERFLOW and flat plate skin friction was consistent for all the configurations analyzed and presents an area for possible investigation.

As stated earlier all of the OVERFLOW cases were run with the one-equation Baldwin-Barth turbulence model. Recently a new version of OVERFLOW was released with the one-equation Spalart-Allmaras model. This version was run on the current OVERFLOW wing/body grid and the different turbulence model was found to give nearly identical skin friction values (.06 count different). All calculations have used all turbulent no-slip surfaces (no laminar run).

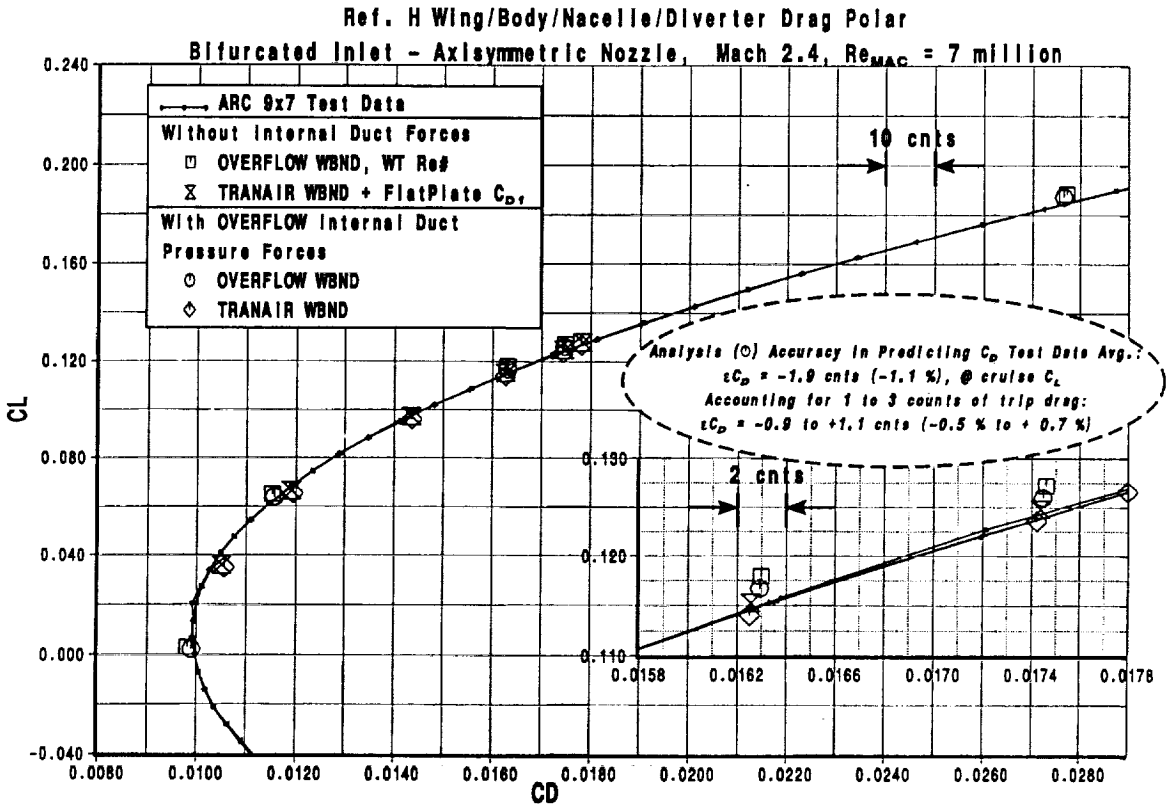

A drag polar for the captive bifurcated installation is shown. After the internal duct correction the bifurcated nacelle OVERFLOW prediction was 2 counts less than test data.

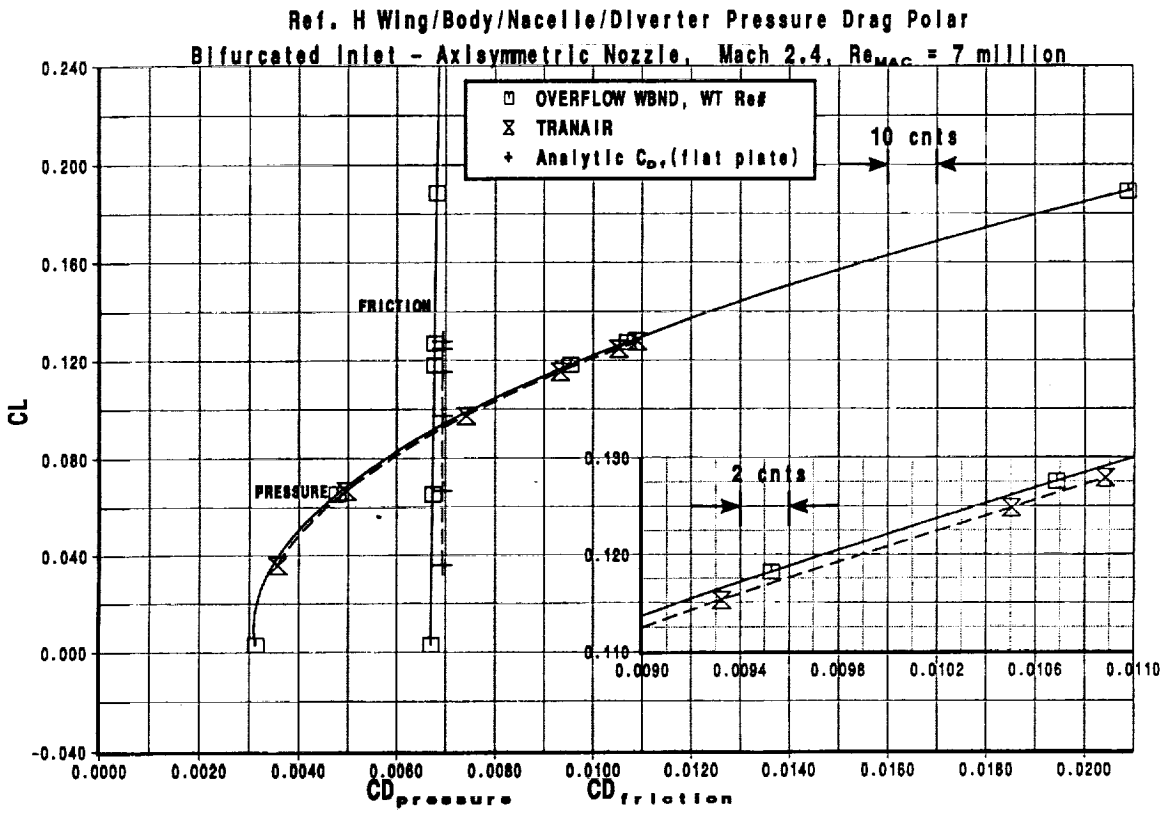

The pressure drag polar plot shown here indicates the same trends as seen for the axisymmetric configuration pressure drag polar shown previously. TRANAIR results were about 1.5 counts higher than OVERFLOW at constant lift.

HSCT High Speed Aerodynamics

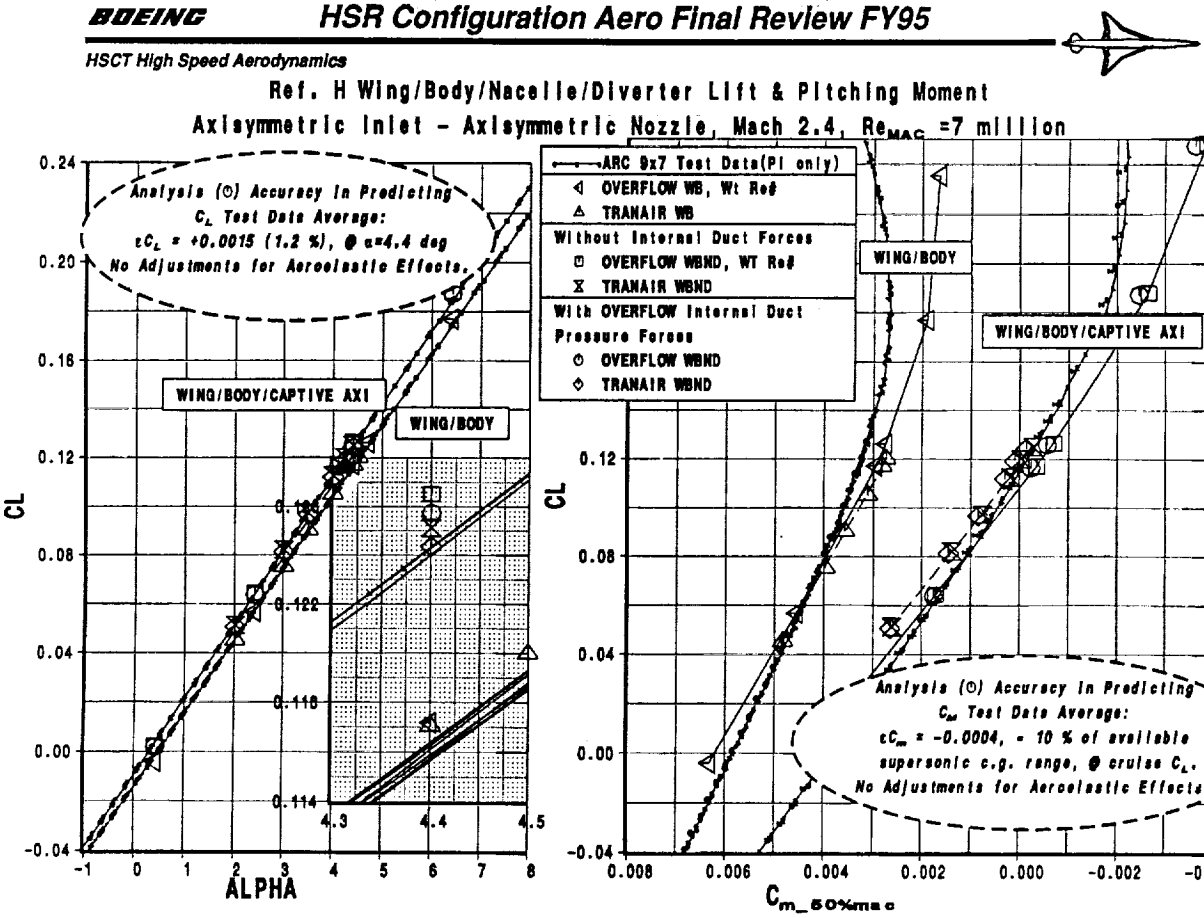

The lift force and pitching moment predicted by TRANAIR and OVERFLOW are shown in this figure for the captive axisymmetric installation. After the nacelle internal duct correction was made the OVERFLOW prediction was found to be about the same amount higher than test than the wing/body alone data (1.2% of cruise lift). This delta was attributed to aeroelastic effects in the wind tunnel data. The CFD results had what appears to be a moment center shift compared to test data for both wing/body and wing/body/nacelle. A portion of this was due to the aeroelastic effect discussed for the lift force comparison (the wing tips in the test are unloading, behind the moment center, resulting in less nose down moment). At the cruise point the OVERFLOW analysis was 0.0004 less than the test data. For a supersonic available c.g. range of 3% of MAC, this error was equivalent to about 10% of available c.g. range. The accuracy requirement of 1% of available c.g. range would be a pitching moment error of 0.00004. This may be an unobtainable level of accuracy. This requirement should probably be loosened in its absolute pitching moment accuracy to 10% of available c.g. range, and a pitching moment slope accuracy specified. The latter will require resolution of the pitching moment rotation seen in all the CFD to test comparisons.

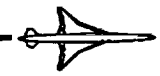

HSCT High Speed Aerodynamics

Ref. H Wing/Body/Nacelle/Diverter Lift & Pitching Moment

Bifurcated Inlet - Axisymmetric Nozzle, Mach 2.4, Re_{MAC} =7 million

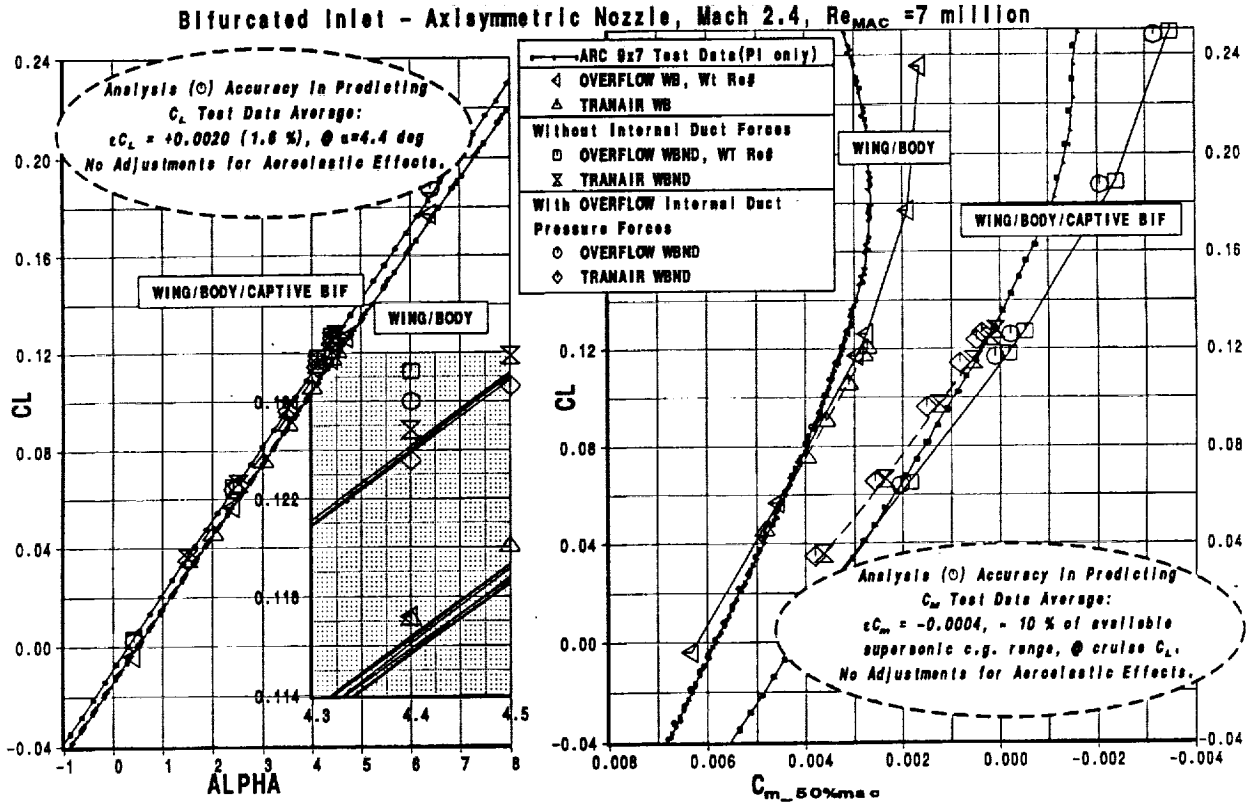

The captive bifurcated lift and pitching moment results are shown. The bifurcated nacelle OVERFLOW prediction was 1.6% higher than than the test data and indicated the same pitching moment trends as seen for the axisymmetric.

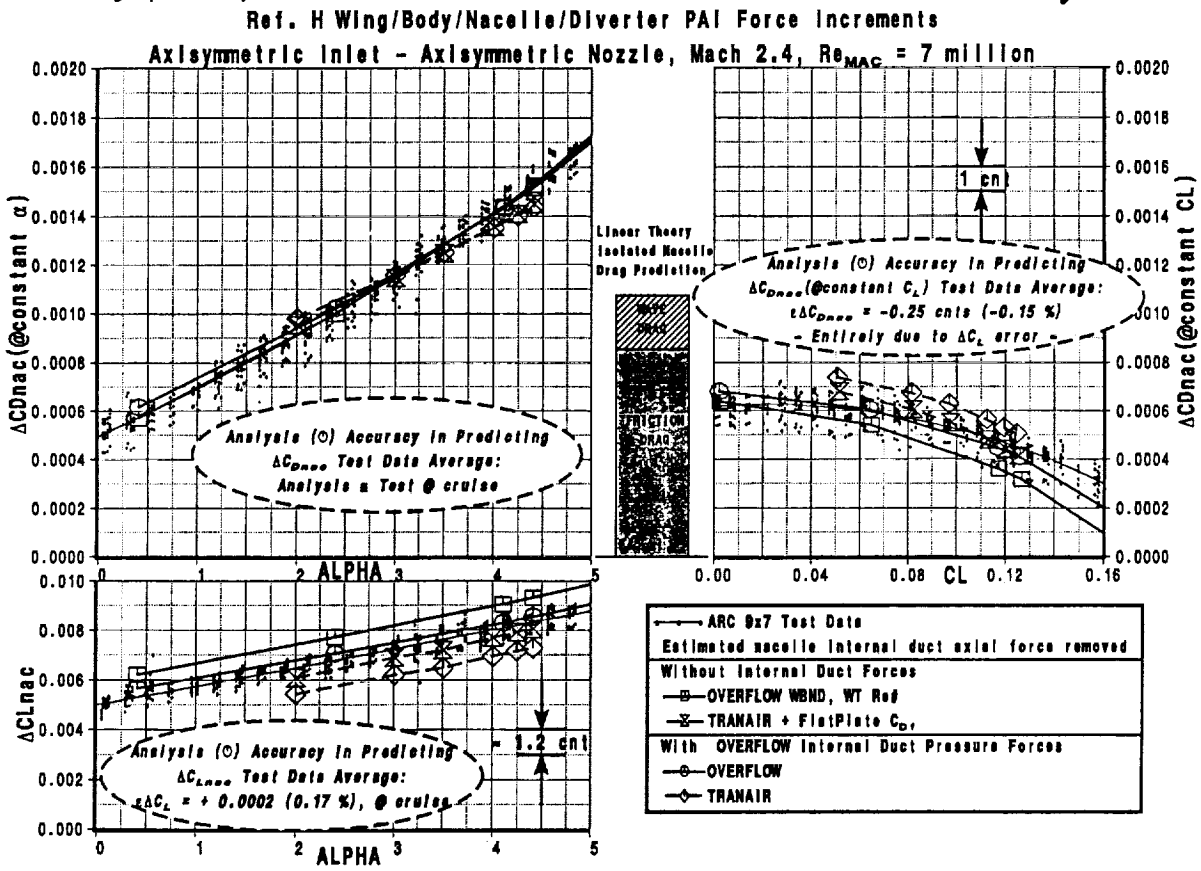

Nacelle force increments are shown for the axisymmetric inlet nacelle. In the upper plot on the left the wing/body drag was subtracted from the wing/body/nacelle/diverter drag at the same angle of attack; the lower figure was obtained through a similar calculation for lift. The figure on the right was obtained by subtracting the wing/body drag from the wing/body/nacelle/diverter drag at the same lift value. This last increment yields the installed nacelle drag at a given lift coefficient and represents essentially the value obtained from the upper left plot minus the lift interference drag from the lower left plot, i.e. the lift gained through installing the nacelles allows the airplane angle of attack to be lowered while still obtaining the same lift as for wing/body. Lift and drag traded this way are essentially proportional to the lift over drag ratio for small movements on the drag polar around the cruise point. The installed axisymmetric nacelle drag increment measured in the wind tunnel test was 4.7 counts (@ CL=.117). Note that this is approximately equal to the drag value from the upper left (15.2 counts @ 4.4 deg) minus the lift benefit from the lower left (0.0084/8 = 10.5 counts). It is also interesting to note that the nacelles can be installed for a drag increment less than isolated skin friction of the nacelles.

The OVERFLOW analysis predicted a nacelle drag increment (at constant angle of attack) that was essentially equal to a curve fit of the test data The predicted lift increment was higher than test by 0.17 % of cruise lift. The drag increment at constant lift (4.4 counts) was lower than test by 0.15 % of cruise drag and came entirely from the lift error. The OVERFLOW increments discussed here are with the internal duct pressures included in order to simulate the wind tunnel data.

HSCT High Speed Aerodynamics

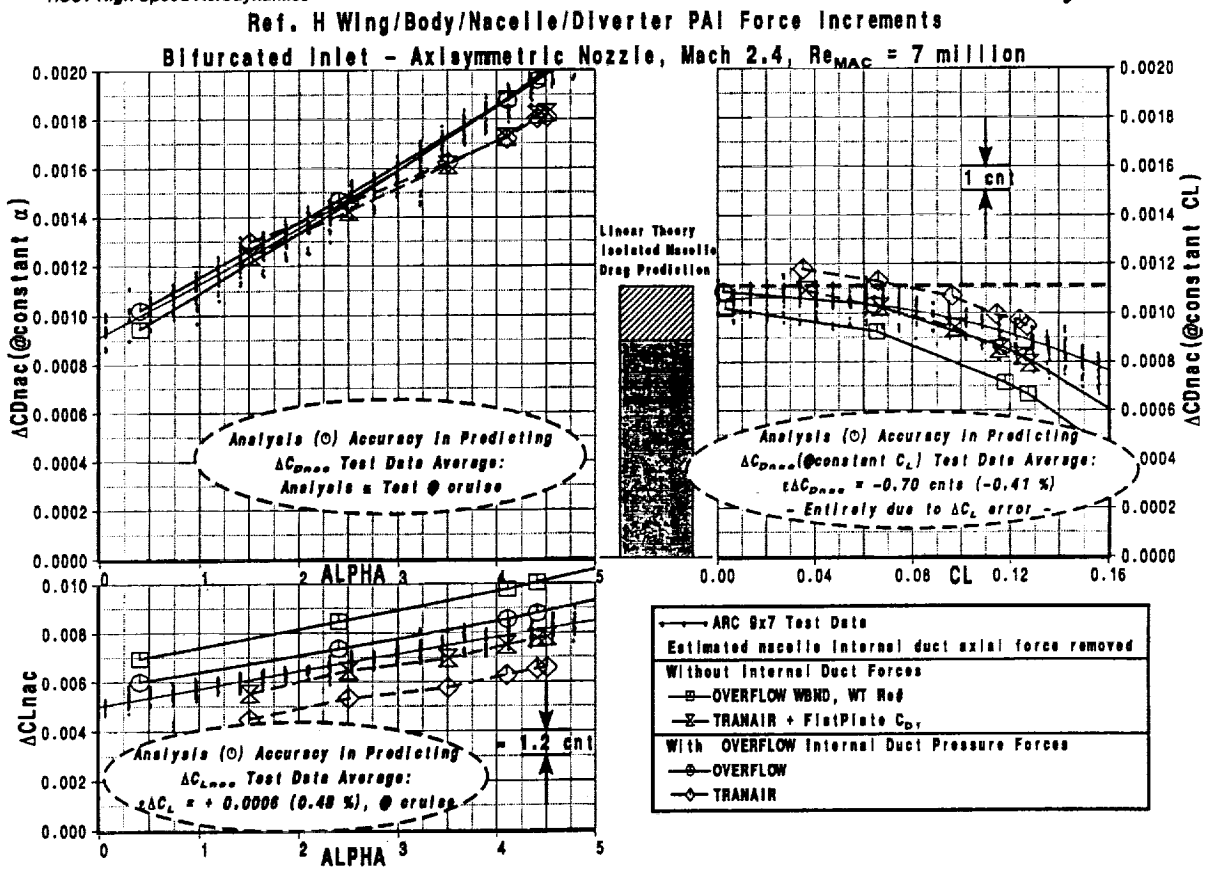

Both TRANAIR and OVERFLOW were not as accurate predicting the bifurcated nacelle force increments. TRANAIR in particular was low in predicting both drag and lift at constant angle of attack; but the effects are cancelling and the installed drag force increment was not as far off. OVERFLOW again predicted the drag increment at constant angle of attack almost exactly. The lift prediction was higher than test (as for the axisymmetric) by 0.48 % of cruise lift. The measured installed nacelle drag increment was 9.3 counts (@ CL=.117). The OVERFLOW value was 8.7 counts which was lower than test by 0.41 % of cruise drag.

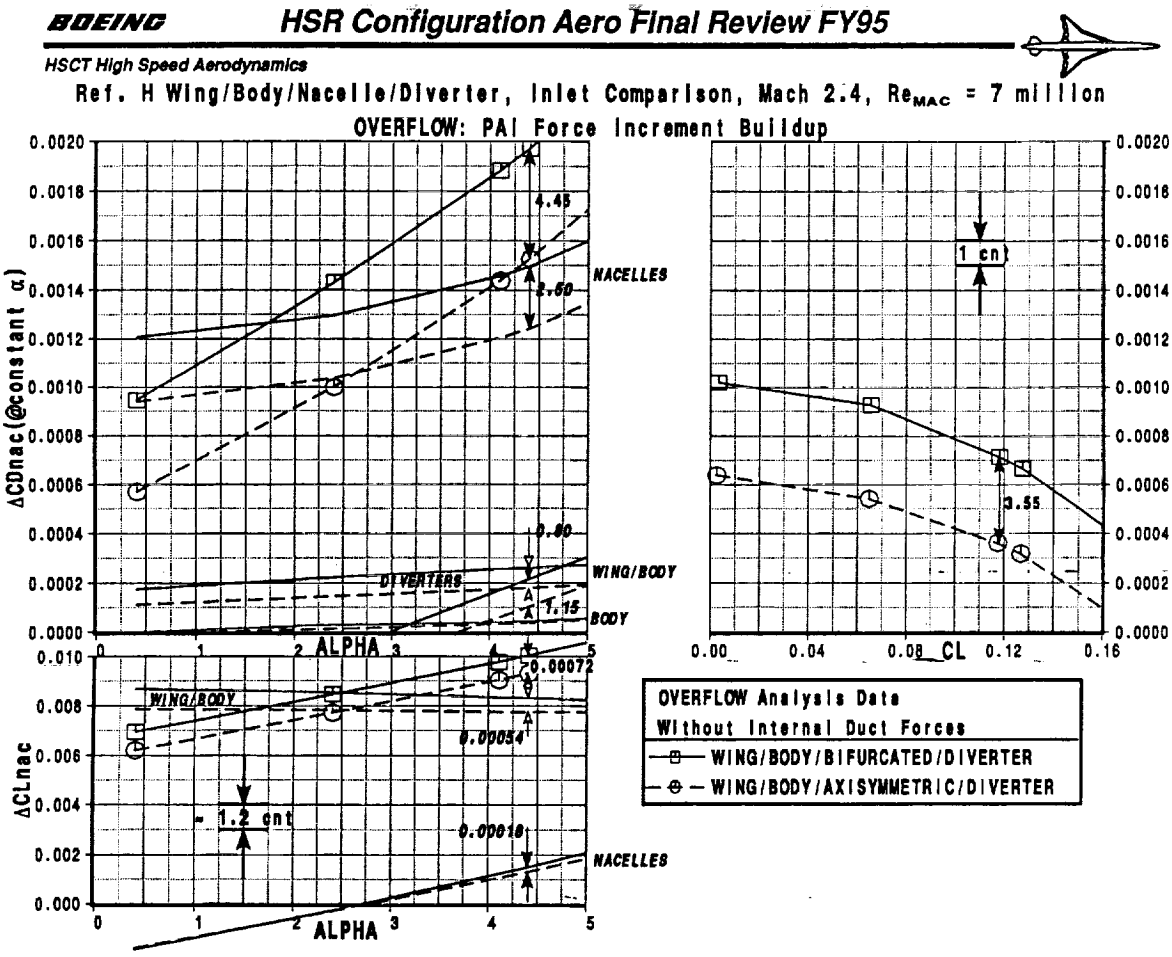

In this next section the difference between the bifurcated and axisymmetric inlet nacelles as measured in the wind tunnel (9.3 - 4.7 = 4.6 counts) and predicted by OVERFLOW (8.7 - 4.4 =4.3 counts) are discussed. As seen in the preceding section it appeared that OVERFLOW was capturing the flow features important to the nacelle installation and predicting the forces and moments accurately as well. The advantage of the CFD solution over the test data was that individual components and flow features could be examined in some detail. This capability was utilized in this section to investigate the bifurcated / axisymmetric drag difference.

The figure shows the nacelle force increments for the two types of nacelles as predicted by OVERFLOW. These data do not have the internal lift forces included as these tend to confuse the comparisons and in realistic installation the inlet would be aligned with the underwing flowfield such that a flow through nacelle would not have internal lift forces. The result was that the installed drag difference between the nacelles dropped from 4.3 to 3.55 counts. The difference was due to the different locations and cross sections of the inlets in the underwing flowfield causing different amounts of lift to carried by the internal ducts of the two nacelle types.

The drag difference between the two nacelles at constant angle of attack was shown to be made up primarily of the drag on the nacelles themselves (2.5 counts) in addition to approximately a count each for the diverters and the wing.

The lift difference between the two nacelles is due to higher lifting pressures on the wing lower surface for the bifurcated installation and a slightly higher nacelle lift for the bifurcated.

Ref. H Wing / Body / Nacelle / Diverter, Inlet Comparison, Mach 2.4, ReMAC = 7 million
OVERFLOW: Bifurcated - Axisymmetric Component Drag Increments @ Alpha=4.4 deg

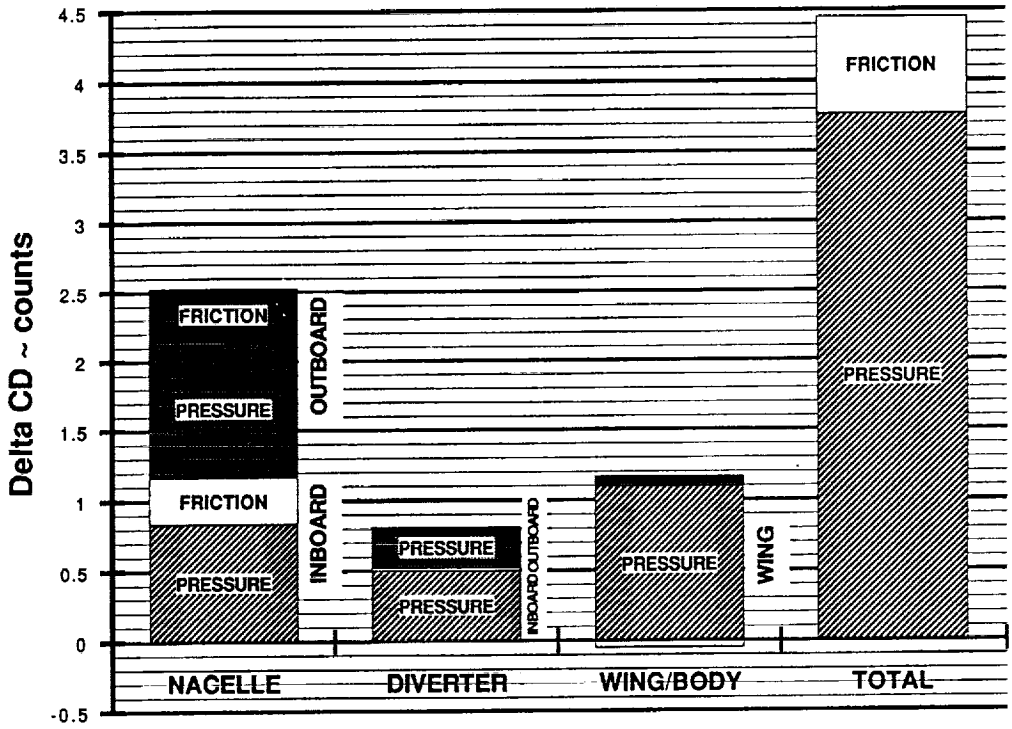

In the figure below the drag difference between the two nacelles at angle of attack of 4.4 degrees was broken down into pressure and friction components. The nacelle delta was found to be composed of 0.7 counts of friction drag (due to the increased length of the bifurcated) and 1.8 counts of pressure drag (primarily from the bifurcated inlet lip bevel).

Both inboard and outboard bifurcated nacelle diverters had increased pressure drag and a very small difference in friction drag over the axisymmetric. This was partially due to the taller diverter for the bifurcated (difficulties with bifurcated installation resulted in diverter height about twice what required; discussed in configuration definition section above). However, as subsequent figures will show the bifurcated diverter also had a substantially larger high pressure region on the forward facing ramp, probably due to lip bevel pressures.

The wing/body drag difference was nearly all due to increased drag on the wing lower surface with the bifurcated installation. There was a small negative friction delta due to larger diverter area cut out of wing lower surface for the bifurcated, and a small pressure drag increment on the body. The wing increment was probably primarily due to the larger extent of the diverter shoulder expansion pressures sucking back on the wing reflex (in the bifurcated installation the diverter shoulder was located farther forward).

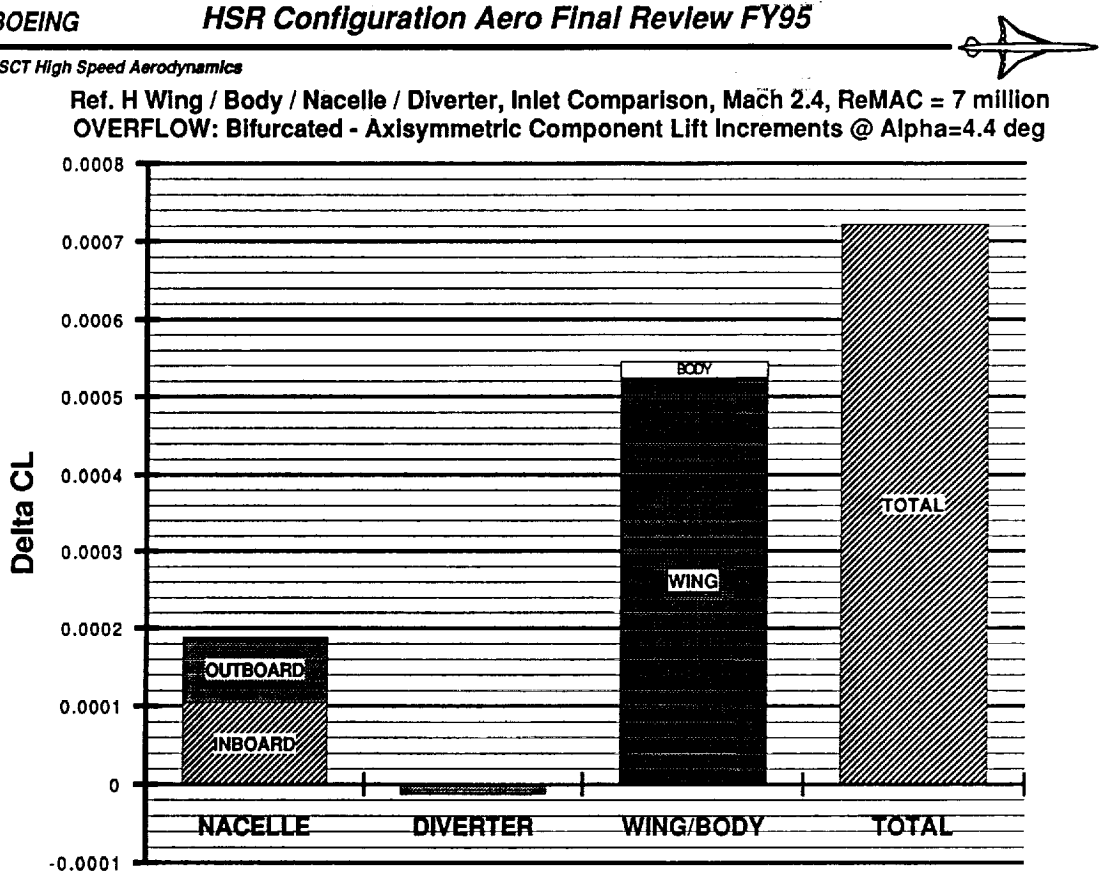

The breakdown of the lift differences between the bifurcated and axisymmetric nacelles is shown. As discussed earlier, the additional lift for the bifurcated installation was due primarily to the wing, with an additional amount split equally between the two nacelles.

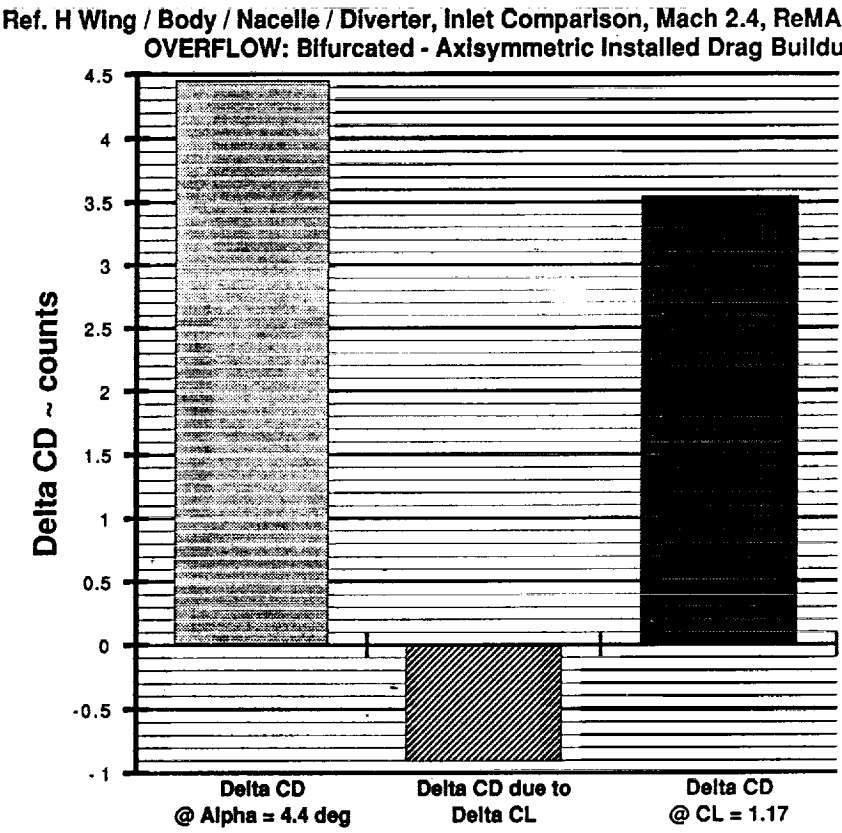

In this figure the delta lift from the previous figure has been converted into a drag increment and summed with the drag delta at constant angle of attack to show how the installed drag delta between the bifurcated and axisymmetric nacelles can be obtained.

Ref. H Wing/Body/Nacelle/Diverter Inlet Comparison, Mach 2.4, Re_{MAC} = 7 million
OVERFLOW: Inboard Nacelle Pressure Contours @ α = 4.4 deg

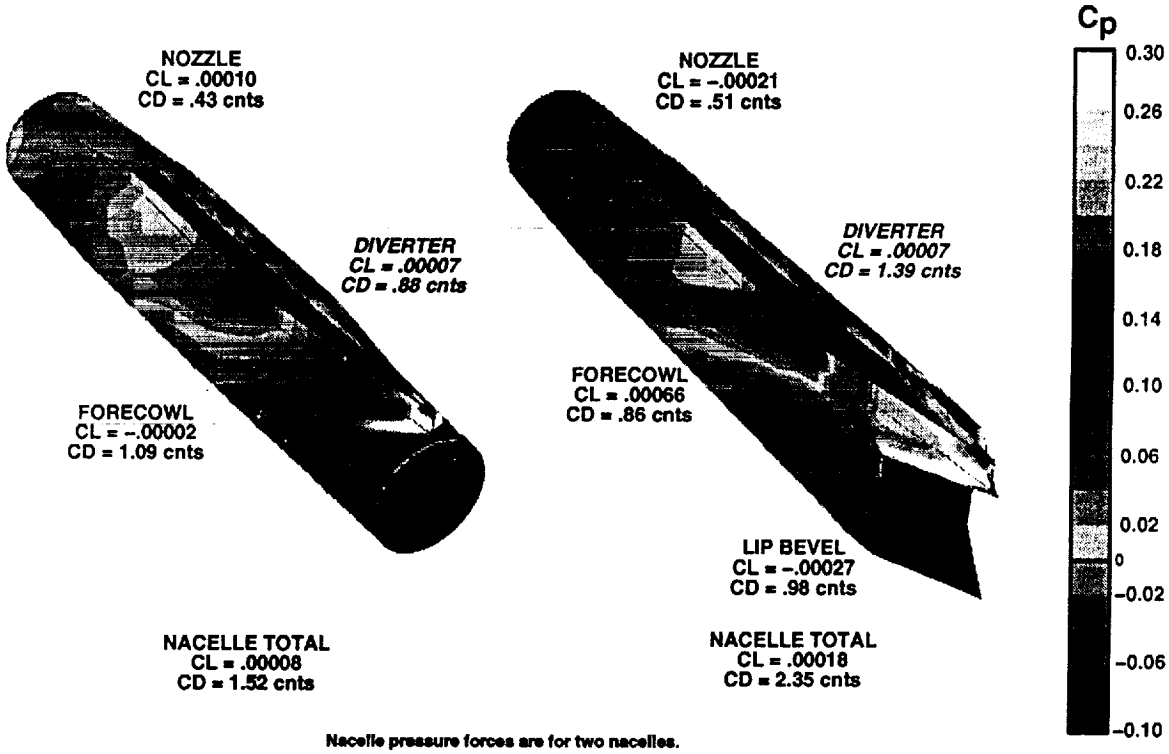

Nacelle pressure forces are for two nacelles.

This figure shows the inboard nacelle surface pressures for the two nacelle types along with the integrated pressure forces for individual nacelles components. An observation of the bifurcated lifting forces shows how the nacelle had large force swings moving aft from the lip bevel: the lip bevel carried negative lift, the forecowl carried positive lift, the nozzle carried negative lift. In addition, the bifurcated nacelle nozzle carried substantially less lift than the axisymmetric nacelle nozzle; this was evident in the pressures on the top of the nozzle (as well as, on the nozzle lower surface as discussed previously). The lift difference between the two nozzles (CL=-0.00031) has been attributed to the small geometry differences discussed earlier and is equivalent to 0.4 counts of drag. The increased diverter drag is clearly seen to be primarily the result of a much larger extent of high pressure on the forward facing ramp; this is due to interference with the lip bevel pressure field.

Ref. H Wing/Body/Nacelle/Diverter Inlet Comparison, Mach 2.4, Re_{MAC} = 7 million
OVERFLOW: Outboard Nacelle Pressure Contours @ α = 4.4 deg

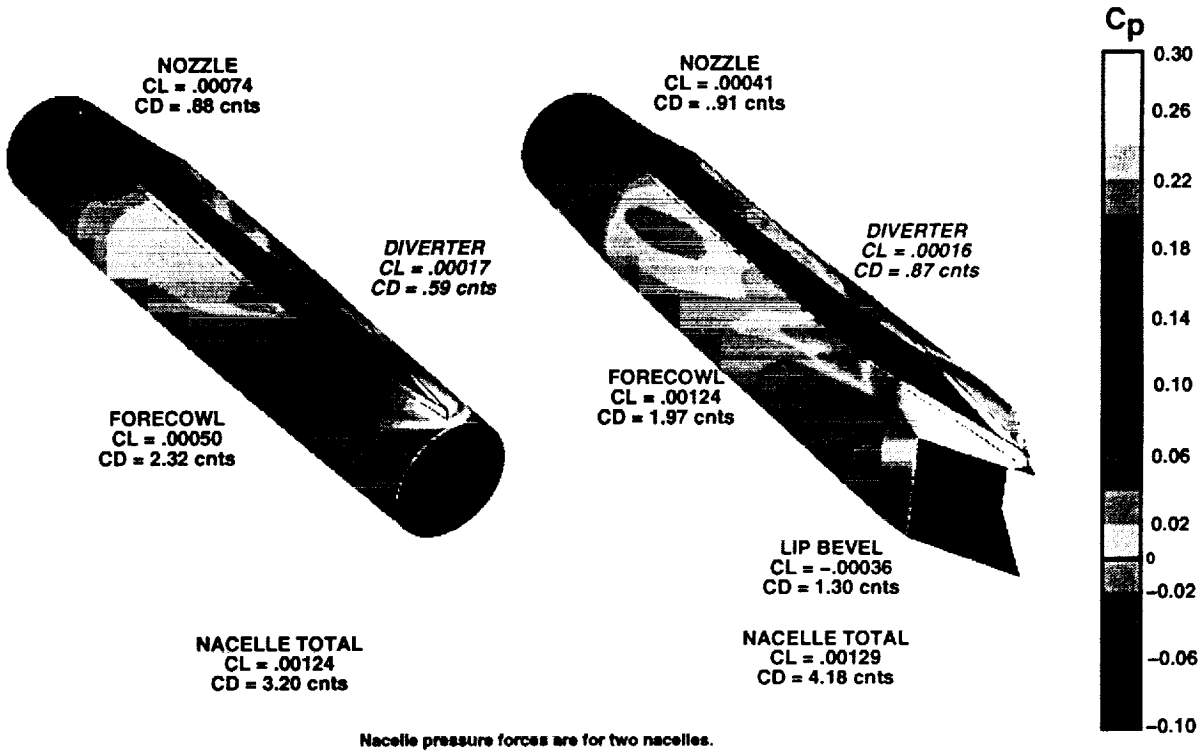

Nacelle pressure forces are for two nacelles.

The outboard nacelle pressure distribution and force components are compared in the figure. The nozzle lift difference (CL=-0.00033) was equal to the inboard value which was equivalent to an additional 0.4 counts of drag difference on the bifurcated nacelle. The implication of these lift differences was that if the nacelles had been built with identical nozzles the drag difference between the two nacelle types would have been reduced by 0.8 counts.

Bifurcated - Axisymmetric Inlet Drag Delta

- Mach 2.4, Supersonic Cruise C_L = 0.12
- Reference H Wing/Body, Bifurcated and Axisymmetric Inlets, Axisymmetric Nozzle

DESCRIPTION	C_D, counts			SOURCE
BIFURCATED - AXISYMMETRIC DRAG DELTA	4.6			Test: 2.7% Ref H @ARC 9x7
• Internal Duct Lift Differences	- 0.7			Overflow: N-S simulation (test Re#)
• Nozzle Geometry Difference	- 0.8			Overflow
CORRECTED BIF - AXI DRAG DELTA	3.1			
• Bifurcated Inlet Lip Bevel	0.5	⇒	0.5	Tranair(ΔC_D=2cnts,ΔC_{D_L}=-1.5cnts)
• Diverter Height & Location	0.5	⇒	0.0	Estimate (Overflow)
• Wing Reflex + Misc Interference	1.4	⇒	1.0	Estimate (Overflow)
• Friction Drag	0.7	⇒	0.7	Overflow
REDUCTION IN BIF - AXI DRAG DELTA	3.1	⇒	2.2,	Range ≈ 1.5 to 2.5 cnts

In summary, the original bifurcated-axisymmetric inlet drag delta of 4.6 counts can be modified with the results from the OVERFLOW analysis:

Measured delta	4.60 counts
Internal lift correction	- 0.70
Dissimilar nozzles	- 0.80
New delta	3.10 counts

This delta is composed of increased diverter pressure drag, increased wing pressure drag, lip bevel drag, and a nacelle skin friction drag increment (0.7 counts). The current lip bevel has about 2 counts of pressure drag, but internal Boeing IR&D studies have shown that it also increases the lift on the wing to such a degree that the drag reduction of going to a bevel-less geometry only reduces the drag by 0.5 counts. However, this reduction is probably not available as the propulsion design team reports that the current lip bevel angle of 4 deg may by a minimum. Moving the bifurcated diverter LE aft will have multiple effects: it appears that the diverter could be moved out of the high pressure region near the lip bevel, the expansion from the diverter shoulder would cover a smaller region on the wing lower surface (good for drag and lift), and the disturbance from the diverter LE would no longer be ingested by the inlet. If, in addition, the wing was reflexed to match the nacelle installation (less reflex than Ref. H) the diverter height could be reduced.

It has been estimated that the minimum level that the bifurcated-axisymmtric increment could be driven down to from the 3 count level above is 1.5 to 2.5 counts (equal to the 0.7 friction delta plus 0.8 to 1.8 counts of nacelle & installation effects).

CONCLUSIONS & RECOMMENDATIONS

- CFD to test comparisons indicate that OVERFLOW provides accurate absolute and incremental aerodynamic data for PAI investigations.
  - Recommend resolving CFD - flat plate skin friction drag discrepancies.
  - Recommend resolving experimental data uncertainties: trip drag level, accounting process for internal duct lift forces, and aeroelastic effects.
- Current Bifurcated-Axisymmetric inlet drag difference adjusted from 4.6 to 3.1 cnts as result of OVERFLOW to test data comparisons:
  - * -0.7 cnts due to internal lift correction,
  - * -0.8 cnts due to dissimilar nozzles.
  - Recommend that all future configurations align inlet with underwing flow field and/or do pretest estimates of internal duct lift.

CONCLUSIONS & RECOMMENDATIONS

- Estimated bifurcated inlet drag penalty 1.5 - 2.5 cnts.
  - Axisymmetric Nozzle.
  - Several additional analyses required to confirm this delta on Reference H.
    * Diverter moved aft on bifurcated installation.
    * Wing lower surface modified for bifurcated.
- No bifurcated inlet work in CA on TCA in 1996.
  - Inlet downselect Nov 1 will use 2 cnts unless additional work done to properly install bifurcated on TCA wing and develop 2D nozzle effects.